Published in final edited form as:
J Comp Neurol. 2013 July 1; 521(10): 2373–2397. doi:10.1002/cne.23291.

Forebrain GABAergic projections to locus coeruleus in mouse

Eugene L. Dimitrov[1], **Yuchio Yanagawa**[2], and **Ted B. Usdin**[1]

[1]Section on Fundamental Neuroscience National Institute of Mental Health 35 Convent Drive, Bethesda, MD 20892, USA

[2]Department of Genetic and Behavioral Neuroscience Gunma University Graduate School of Medicine and JST, CREST 3-39-22 Showa-machi, Maebashi 371-8511, Japan

Abstract

The noradrenergic locus coeruleus (LC) regulates arousal, memory, sympathetic nervous system activity and pain. Forebrain projections to LC have been characterized in rat, cat and primates, but not systematically in mouse. We surveyed mouse forebrain LC projecting neurons by examining retrogradely labeled cells following LC iontophoresis of fluorogold and anterograde LC labeling after forebrain injection of biotinylated dextran-amine or viral tracer. Similar to other species, the central amygdalar nucleus (CAmy), anterior hypothalamus, paraventricular nucleus, and posterior lateral hypothalamic area (PLH) provide major LC inputs. Using mice expressing green fluorescent protein in GABAergic neurons we found that more than one.third of LC projecting CAmy and PLH neurons are GABAergic. LC colocalization of biotinylated dextran-amine, following CAmy or PLH injection, with either green fluorescent protein or GAD65/67-ir confirmed these GABAergic projections. CAmy injection of adeno.associated virus encoding channelrhodopsin-2-Venus showed similar fiber labeling and association with GAD65/67-ir and tyrosine hydroxylase-ir (TH-ir) neurons. CAmy and PLH projections were densest in a peri-coerulear zone, but many fibers entered the LC proper. Close apposition between CAmy GABAergic projections and TH-ir processes suggests CAmy GABAergic neurons may directly inhibit noradrenergic principal neurons. Direct LC neuron targeting was confirmed by anterograde transneuronal labeling of LC TH-ir neurons following CAmy or PLH injection of a herpes virus that expresses red fluorescent protein following activation by Cre recombinase in mice that express Cre recombinase in GABergic neurons. This description of GABAergic projections from CAmy and PLH to the LC clarifies important forebrain sources of inhibitory control of CNS noradrenergic activity.

Keywords

Noradrenergic; Forebrain; Brainstem; GAD67-GFP knockin; anatomical tract tracing

Correspondence: T. B. Usdin, Section on Fundamental Neuroscience, National Institute of Mental Health, 35 Convent Drive, Bethesda, MD 20892, USA, telephone 301-402-6976, fax 301-402-0245, usdint@mail.nih.gov.

Conflicts of interest: None of the authors have any conflict of interest.

Introduction

Neurons of the locus coeruleus (LC) project throughout much of the central nervous system (Dahlstroem et al., 1964; Fallon et al., 1978). The function of these noradrenergic projections can be viewed globally as optimizing behavioral performance (Berridge and Waterhouse, 2003; Aston-Jones and Cohen, 2005) or more specifically as modulating processes such as attention (Gompf et al., 2010), sleep-waking cycle (Aston-Jones and Bloom, 1981), autonomic functions (Sved and Felsten, 1987; Miyawaki et al., 1991), or nociception (Wei et al., 1999), depending upon the projections considered. LC function is regulated by major afferents from several brainstem nuclei and limbic regions (Cedarbaum and Aghajanian, 1978; Luppi et al., 1995; Lee et al., 2005; Verret et al., 2006; Sirieix et al., 2012). It is important to characterize these projections in mice because of the increased use of mice to investigate circuit function and create disease models.

In several species, particularly rat and nonhuman primate, it has been demonstrated that major forebrain inputs to the LC and pericoerulear area (Peri-LC) are provided by the central amygdala (CAmy) (Hopkins and Holstege, 1978; Price and Amaral, 1981; Price, 1986; Wallace et al., 1989), and hypothalamic areas that include the paraventricular nucleus (PVN) (Geerling et al., 2010), lateral hypothalamus (Saper et al., 1979), especially the posterior lateral hypothalamus (PLH) (Peyron et al., 1998; Puskas et al., 2010), ventromedial hypothalamus (Saper et al., 1976) and particularly by preoptic regions (Luppi et al., 1995; Steininger et al., 2001; Lee et al., 2005) including the ventrolateral preoptic region (Steininger et al., 2001) as well as the anterior cingulate cortex (Gompf et al., 2010). However, several studies report little or no CAmy input to the core LC and suggest the CAmy projections to the Peri-LC may target either distal dendrites of LC neurons or other cells, such as those of the Barrington nucleus (Luppi et al., 1995). The neurotransmitter content of LC afferents has been partially described in several species, however relatively little information is available for mouse. Major excitatory forebrain inputs are thought to include hypocretin/orexin neurons widely distributed in the lateral hypothalamus (Peyron et al., 1998; Horvath et al., 1999; Gompf and Aston.Jones, 2008; Henny et al., 2010) and potentially a glutamatergic/dynorphin containing projection from the CAmy (Reyes et al., 2011). Inhibitory forebrain inputs include enkephalin containing projections from the CAmy (Van Bockstaele et al., 2001). GABAergic projection neurons from the CAmy are thought to provide an input to brainstem regions that include the LC (Swanson and Petrovich, 1998; Tasan et al., 2010). However, this is largely inferred from the high density of GABA neurons in the CAmy (Poulin et al., 2008), the projection of CAmy neurons to the LC (Cedarbaum and Aghajanian, 1978; Wallace et al., 1989), and the existence of synapses that CAmy efferents, or afferents from other unknown sources, make with tyrosine hydroxylase (TH) containing dendrites that appear asymmetric by electron microscopy (Van Bockstaele et al., 1996; Van Bockstaele, 1998). PLH GABAergic projections to the LC have been suggested to be part of the circuitry controlling sleep-wake function (Verret et al., 2006).

Modulation of LC activity may be mediated through projections to a pool of GABAergic neurons in the Peri-LC (Aston.Jones et al., 2004) or by direct connections to LC noradrenergic principal neurons. Early anatomical studies in rat suggested that some brainstem afferents terminate within the LC proper, while most other projections target the

Peri-LC (Aston-Jones et al., 1986; Van Bockstaele et al., 2001). In addition it has been demonstrated that some projections from the preoptic and lateral hypothalamic areas, periaqueductal gray, and CAmy target the LC core (Luppi et al., 1995; Lee et al., 2005; Reyes et al., 2011), although some of the lateral hypothalamic hypocretin neurons may target non-noradrenergic LC projection neurons (Del Cid-Pellitero and Garzon, 2011). However, for many afferents it is still not clear whether they target interneurons or dendrites of noradrenergic neurons within the Peri-LC zone.

The goals of this study were to survey the forebrain projections to the mouse LC with particular emphasis on the major forebrain GABAergic innervation of the nucleus. We iontophoretically injected the retrograde tracer fluorogold (FG) into the LC of a mouse line in which green fluorescent protein (GFP) is genetically targeted to GABAergic neurons (Tamamaki et al., 2003) and identified retrogradely labeled neurons. We identifed a large number of forebrain GABAergic projection neurons, based on colocalization with GFP. We then used biotinylated dextran amine (BDA) and an adeno-associated virus encoding a channelrhodopsin-2-Venus fusion (ChR2-Venus) in combination with labeling by antibodies to GAD65/67 or GFP to confirm the major GABAergic forebrain projections. Finally, support for direct connection between forebrain GABAergic projection neurons and LC noradrenergic cells was provided by transneuronal anterograde labeling of LC principal neurons following CAmy and PLH injection of a herpes simplex 1 virus (HSV1) H129 strain with Cre recombinase dependent marker expression (Lo and Anderson, 2011) in mice that express Cre recombinase (Vong et al., 2011) and GFP in GABAergic neurons.

Materials and Methods

Animals

All procedures were approved by the National Institute of Mental Health Animal Care and Use Committee and were in accordance with the Institute for Laboratory Animal Research *Guide for the Care and Use of Laboratory Animals.* Mice were housed under a 12/12 hour light/dark cycle (lights on at 6:00 am) with free access to food and water. Female mice between 80 and 140 days of age and weighing from 21 to 25 grams were used for all experiments. The animals were singly housed following stereotaxic surgery. C57Bl/6J (Jackson Laboratories, Bar Harbor, ME), GAD67-GFP (Δneo) knock-in mice (Tamamaki et al., 2003) (referred to as GAD67-GFP), and mice with Cre recombinase knocked into the vesicular GABA transporter locus ($Vgat^{ires\text{-}Cre/+;}$) (Vong et al., 2011) and a Cre recombinase dependent GFP in the ROSA26 locus (RCE:LoxP) (Sousa et al., 2009) referred to as VGAT-iCre/LSGFP were used.

Antibody Characterization

Fluorogold—Antibody specificity was verified by the absence of labeling in animals not injected with fluoro-gold.

GAD65/67—According to the manufacturer the antibody recognizes bands of ~65kDa and ~67kDa on Western blots that correspond to GAD65 and GAD67.

GFP—Antibody specificity was verified by the absence of labeling in animals that do not genetically express GFP.

TH—According to the manufacturer the antibody exclusively recognizes a 60 kDa band corresponding to TH on Western blots of a PC12 lysate and produces strong labeling of mouse substantia nigra by immunohistochemistry. We observed strong labeling of cells in the LC and in other brainstem nuclei that correspond to established catecholamine cell groups.

NeuN—. According to the manufacturer the antibody labels a neuronal specific DNA binding nuclear protein called NeuN (Neuronal Nuclei). The antibody exclusively labels neuronal nuclei and perikarya of the mouse CNS and PNS.

Secondary antibodies—Fluorophore and biotin coupled secondary antibodies raised in donkey and absorbed to remove cross reactivity with immunglobulins from unintended species were obtained from Jackson ImmunoResearch (West Grove, PA).

Tracer Injection

Animals were anesthetized with isoflurane and placed in a stereotaxic apparatus. A longitudinal skin incision and removing pericranial connective tissue exposed the bregma and lambda sutures of the skull. A 10 to 15 μm diameter glass micropipette was inserted into the desired brain structure via drilled holes and the tracer was delivered ionophoretically using 5 μA positive pulsed current for 10 minutes (BAB-500 iontophoresis pump, Kation Scientific, Minneapolis, MN). The micropipette was left in position for 5 minutes after the infusion. The same method was used for delivery of both 1% FG (Invitrogen, Carlsbad, CA) and 10% BDA (InVitrogen) in sterile saline. The coordinates were (relative to bregma) anteroposterior −5.4 mm, lateral + 0.8 mm and dorsoventral – 4.0 mm for the LC, − 1.5 mm, + 2.4mm – 5.0 mm for the CAmy and − 1.6 mm, + 1.2 mm and – 5.0 mm for the PLH. Adeno-associated virus encoding ChR2-Venus (AAV2/1.CAG.ChR2-Venus.W.SV40, 10e12 particles/ml, Penn Vector Core, Philadelphia, PA) and Herpes simplex 1, strain H129 encoding Cre recombinase dependent red (tandem dimer Tomato) fluorescent protein (H129DTK-TT(tdT HTK) (Lo and Anderson, 2011), referred to as HSV1-H129-LStdT, were injected into the CAmy or into the PLH by pressure (Microsyringe pump, World Precision Instruments, Inc, Saratoga, FL) in a volume of 0.1 μl over 5 minutes. All animals were given analgesic and fluids for three days after the surgery.

Ten days after the stereotaxic injection for FG, 10 days to four weeks for BDA, 28 days for ChR2-Venus, and 24-72 hours for HSV1-H129-LStdT, the animals were deeply anesthetized, perfused with fixative, and the brains were removed and processed for immunohistochemistry.

Immunohistochemistry

FG detection—The animals were perfused with 4% paraformaldehyde and 30 μm sections were cut using a vibrating microtome and collected as three consecutive sets, each set containing nonconsecutive sections separated by 60 μm. The free floating sections were

incubated with a 3% hydrogen peroxide followed by incubation in blocking solution containing 0.5% triton X-100 and 3% normal donkey serum for two hours. After the blocking step the sections were incubated in anti-FG rabbit antibody overnight, and incubated in DyLight 568 anti–rabbit (1:400) for 5 hours on the next day. This FG immunolabeling was followed by visualization of GFP-ir by incubation in chicken anti-GFP primary antibody overnight followed by incubation in CY5 anti-chicken (1:400 dilution). A double immunostaining with anti-NeuN (mouse, 1:500 dilution, Millipore, Temecula, CA), followed by DyLight 594 anti-mouse (1:400) and anti.GFP chicken antibody as described above was applied to assess the distribution and approximate number of GFP/GAD67 neuronal population in the CAmy. Brainstem sections used for confirmation of the injection sites were immunolabeled for FG as described above and the fluorescence of GFP in the GAD67-GFP transgenic mice was used for orientation.

BDA labeling—The brainstem was cut on a vibrating microtome into 30 μm sections. The BDA signal was visualized by incubation in streptavidin derivatized horseradish peroxidase (Jackson Immunoresearch) diluted 1:2 000 for 1 hour followed by incubation with DyLight 568 (Pierce, Rockford, Il) or Pacific blue (InVitrogen) conjugated-tyramine. Once BDA was visualized, sections were incubated overnight with a mouse antibody against GAD65/67, which was visualized with an Alexa 647 labeled anti-mouse antibody followed by overnight incubation with chicken anti-GFP antibody detected with a DyLight 488 labeled anti-chicken IgG. Alternatively, following labeling of BDA with peroxidase and visualization with Pacific blue conjugated-tyramine, tissue from wild-type mice was serially incubated with anti-GAD65/67 and anti-TH, which were detected with Alexa 647 and Alexa 594 conjugated antibodies. The anatomical levels of sections and specific regions were identified using the Franklin and Paxinos (Franklin and Paxinos, 2008) atlas. Tyramine derivatives for use as peroxidase substrates were synthesized as described by Hopman et al (Hopman et al., 1998).

AAV-ChR2-Venus detection—The brain sections were obtained as described above. First TH-ir was visualized, using the anti-TH primary antibody at 1:5000 followed by incubation with biotin-labeled anti-sheep antibody and then avidin-biotin-peroxidase complex (ABC Elite reagents, Vector Labs, Burlingame CA) and Pacific blue conjugated.tyramine. Next, the material was labeled with the anti-GAD65/67 mouse antibody, which was detected with an Alexa 647 secondary antibody. ChR2-Venus was directly visualized as yellow, TH-ir as blue, and GAD65/67-ir as far red.

HSV1-H129-LStdT detection in VGAT-iCre/GFP mice—Sections were labeled with the anti-TH antibody as above. GFP and tdTomato were directly visualized as green and red fluorescence.

Image acquisition and processing

Widefield microscopy—Images were obtained on an Olympus IX70 microscope equipped with an X-Cite illuminator (Lumen Dynamics Group Inc. Mississauga, Ontario, Canada) and a Photometrics Cool-Snap FX camera (Photometrics, Inc. Tucson, AZ) using IPLab software (Scanalytics, Rockville MD).

Confocal Microscopy—Fluorescent labeling was detected in representative sections using a Zeiss LSM510 confocal microscope (Zeiss USA, Thornwood NY) in the NINDS Intramural Light Imaging Facility. High magnification images were obtained with a 63X oil objective at 1024 X 1024 pixels (0.14 μm/pixel). Selection of image planes was performed using Volocity (Improvision, Waltham MA). To illustrate cell labeling Z-stacks were projected as overlays. Single optical sections are shown for illustration of fiber and puncta labeling. To quantitatively evaluate colocalization between BDA and GAD65/67-ir, we used the "Quantification" algorithm in Volocity and single optical sections in which BDA was visualized with pacific blue (excitation wavelength 405 nm) and GAD65/67-ir with Alexa 647 (excitation wavelength 650 nm). The maximum and minimum thresholds were set once manually for each channel and the automatic threshold created by the algorithm was used for subsequent images. The "Generate colocalization" command applies Pearson's correlation to calculate colocalization coefficients (My and Mx) that describe the number of pixels over threshold in one channel that colocalize with pixels over threshold in the other channel (Barlow et al., 2010). The results are presented as percent colocalization.

Non-adjacent sections from four animals were used to estimate the number of amygdalar GAD67 projection neurons. The two sections identified at each level had at least 60 μm between them. At the magnification used the full thickness of the section was visualized. Only cells with a clearly visible cell body outline around cell's nucleus were counted. The Lindersrom-Lang/Abercombie equation for estimation of true number of objects in 3-D segments was applied (Abercrombie, 1946; Hendreen, 1998). The cell counts are presented as average per animal plus/minus standard deviation.

Image presentation—Images were transferred from the acquisition software directly or following image plane selection in Volocity to Adobe Photoshop (Adobe Systems Inc, San Jose CA). Contrast and intensity were adjusted and colors changed by moving entire images to different channels. No manipulation of individual image elements was performed.

Results

We identified GABAergic neurons by GFP expression in heterozygous animals from a mouse line in which GFP replaces the sequence of the first coding exon of the mouse GAD67 gene, referred to as GAD67-GFP mice. Expression of GFP by GABA neurons in this line has been well documented (Tamamaki et al., 2003; Brown et al., 2008; Suzuki and Bekkers, 2010; Wang and Bradley, 2010). The mice we worked with are several generations removed from the characterized animals. To confirm the appropriate pattern of GFP expression we first looked at the overall pattern of GFP expressing cells (data not shown). This was similar to that observed previously for GAD67 mRNA by in situ hybridization histochemistry in rat (Esclapez et al., 1993), to that shown for mouse in the Allen Mouse Brain Atlas (Allen, 2009), and for GFP expression in this mouse line in previous studies (Tamamaki et al., 2003). We also performed double labeling using antibodies to GFP and to calbindin and neuropeptide Y. Almost all of the calbindin.ir and neuropeptide Y-ir cells in the amygdala contained GFP-ir (data not shown).

We examined the distribution of GFP expressing cells in the amygdala in more detail (Figure 1). Large numbers of GFP-ir cells were present throughout the amygdala. The centromedial, centrocentral, and centrolateral subnuclei of the CAmy had a much greater density of GFP-ir cells than the neighboring basolateral and lateral nuclei. The greatest density of GFP-ir cells was in densely packed clusters wedged between the CAmy and basolateral nucleus and lateral to the basolateral nucleus that correspond to recently described paracapsular cell groups (Marowsky et al., 2005). We estimated the proportion of neurons in the CAmy that were GABAergic by double labeling with the neuronal nuclear marker NeuN and counting the numbers of labeled cells at one representative level, – 1.34 mm from bregma. The average number of NeuN immunopositive (NeuN-ir) neurons in the CAmy in one hemisection at this level was 623 ± 26.1 and the average number of GFP-ir expressing neurons was 240 ± 16.6, with counts performed on 8 sections from four animals. Thus, at this representative level, 38.6% ± 3.1 of the CAmy neurons defined by NeuN-ir were GABAergic as defined by GFP expression in this GAD67-GFP knock-in mouse.

To label neurons that project to the LC we performed unilateral iontophoretic injections of the retrograde tracer FG into the nucleus in GAD67-GFP mice. In each of the cases used for analysis FG covered the LC proper (defined as the region of dense TH-ir neurons adjacent to the floor of the 4^{th} ventricle) and the Peri-LC dendritic zone (defined as the areas immediately adjacent to the LC proper that contain TH-ir dendrites). FG also spread, with a small amount of variability between cases, into closely adjacent areas that included parts of the Barrington nucleus medially and parts of the mesencephalic trigeminal nucleus and medial parabrachial nucleus laterally (Figure 2). Retrogradely transported FG filled cell bodies of neurons in many forebrain areas that have been documented in rat, cat, and monkey to project to the LC proper or Peri-LC dendritic zone, including the CAmy, PLH, anterior hypothalamic area, PVN, arcuate nucleus, bed nucleus of the stria terminalis, and sensory cortex (see Discussion).

The CAmy contained a large population of retrogradely filled neurons. All subdivisions, centromedial, centrocentral, and centrolateral, contained FG-ir labeled neurons. The number of FG-ir neurons varied with the rostral-caudal level (Figure 3). At each level many of the retrogradely labeled cells contained GFP. Cell counts from the entire CAmy were made at three levels (– 1.06 mm, −1.34 and – 1.58 mm from bregma, two non-consecutive hemisections per level) for a total of six sections per animal from four animals. There was an average of 71 ± 20 FG-ir and 215 ± 15.4 GFP-ir neurons on the side ipsilateral to the injection. An average of 13.7% (28 ± 9.8) of the GFP-ir neurons contained FG while 39.4% ± 7.3 of the FG-ir neurons contained GAD67-GFP-ir. Thus about 40% of the neurons projecting from the CAmy to the LC appear to be GABAergic. Cells containing FG-ir and not GFP-ir and many containing only GFP-ir were intermixed with the double.labeled cells (Figure 3J to L). The side contralateral to the injection contained only a few FG-ir neurons, and these cells did not contain GFP (Figure 4).

The PLH also contained a considerable population of retrogradely labeled cells following FG injection into the LC (Figure 5). The average number of FG labeled neurons in the PLH evaluated in two non-consecutive sections −1.58 mm from bregma was 87 ± 15.8, the average number of GFP-ir neurons was 225 ± 19 and the number of FG/GFP-ir colocalized

neurons was 26 ± 4.4. Thus, in the PLH, about 11.9% ±7.5 of the GABAergic neurons on the ipsilateral side appear to project to the LC and 30.5% ± 4.5 of the LC projecting cells are GABAergic. The PLH contralateral to the injection site also contained FG labeled neurons but their population was much smaller than the ipsilateral group and was confined to the dorsomedial part of the nucleus (Figure 5).

In the hypothalamic area, the ventromedial and ventrolateral preoptic nuclei, medial preoptic area, anterior hypothalamic area, lateral preoptic area, lateral hypothalamic area and bed nucleus of the stria terminalis contained retrogradely labeled cells after iontophoresis of FG into the LC (Figure 6). The number of FG-ir labeled cells in these areas did not reach the number of FG-ir labeled cells in the CAmy and PLH. They were strictly ipsilateral to the injection site. High power images showed a number of GAD67-GFP/FG-ir coexpresing cells in each of these areas (Figure 7). The PVN (Figure 8), arcuate nucleus and somatosensory cortex also showed FG-ir positive cells but without any colocalization with GFP-ir.

Numerous FG labeled cells were also present in medullary nuclei including the nucleus prepositus, lateral paragigantocellular nucleus and neighboring ventral gigantocellularis nucleus (not shown). This observation is consistent with previous studies in other species (Aston-Jones et al., 1991; Luppi et al., 1995).

To confirm the projection of CAmy and PLH GABAergic neurons to the LC we injected the anterograde tracer BDA into the CAmy and PLH (Figure 9) in GAD67-GFP knock-in and in wild-type mice. Representative brain sections were double labeled for BDA and GAD65/67-ir, or BDA and GFP-ir, or triple labeled for BDA and GAD65/67-ir and TH-ir. The LC received BDA containing fibers from both the CAmy and the PLH injections. Following BDA injections into the CAmy, BDA containing fibers followed an ipsilateral descending pathway that occupied somewhat lateral parts of pontine tegmentum in the area of the parabrachial nucleus and LC, and after that reached the nucleus gigantocellularis ventrally and the nucleus of the solitary tract most distally. This general pattern of brainstem labeling by anterograde tracers injected into the CAmy has been well described in rat, cat, and monkey (Hopkins and Holstege, 1978; Price, 1986; Luppi et al., 1995; Van Bockstaele et al., 1996). The most intensely labeled BDA fibers projecting from the CAmy appeared in the region of the medial parabrachial nucleus closely adjacent to the laterodorsal edge of the LC. Sparser, in comparison to the fibers in medial parabrachial nucleus but still numerous, BDA labeled fibers were also present in the area of the TH-ir cell bodies of the LC proper and dispersed among the TH-ir dendrites medial and medioventral to the nucleus, in the Peri-LC dendritic zone (Figure 9 B and C). The mouse LC area has not been described precisely but the areas that receive the bulk of the CAmy efferents may correspond to lateral and rostromedial Peri-LC dendritic zones described in rat (Shipley et al., 1996). BDA injection into the PLH also labeled a number of efferent fibers in the LC area. Overall, the highest fiber concentration was in the ventrocaudal region of the brainstem around the nucleus gigantocellularis. BDA fibers projecting from the PLH were concentrated at the lateral border of LC and throughout the medial parabrachial nucleus with somewhat fewer fibers traversing the nucleus and reaching the Peri-LC rostroventral to the nucleus (Figure 9 E and F).

Next, we focused our attention on the efferent BDA fibers that reached the LC and the Peri-LC dendritic zone, and their possible interaction with TH-ir neurons and dendrites (Figure 10A, B and C). The Peri-LC zone is subdivided into rostromedial paracoerulear, juxtaepidymal and lateral regions in rat (Shipley et al., 1996). High magnification confocal images from the LC proper showed BDA containing fibers closely adjacent to TH-ir neurons (Figure 10D, E and F). Some of the BDA containing fibers had points of apparent contact with TH-ir dendrites in an area that may correspond to the rat rostromedial paracoerulear region (Figure 10G, H and I), demonstrated by colocalized pixels in single optical sections, consistent with the possibility of synaptic contacts between amygdalar efferents and TH-ir dendrites (Figure 10J, K and L). Double labeling also showed that some of the BDA positive fibers in the LC contained GAD65/67-ir in wild-type (Figure 11A to F) and GFP-ir in GAD67-GFP knock-in (Figure 11G to L) mice. An average of 26.9% ± 3.8 of the BDA pixels colocalized with GAD65/67-ir (see Methods for the colocalization procedure). A few puncta in which labeling for BDA, GAD65/67-ir, and TH-ir overlapped were scattered through the Peri-LC zone (Figure 12). These may represent anterogradely labeled GABAergic fibers in close approximation to noradrenergic dendrites. Because fine axonal processes and terminals might be better visualized using a membrane protein as a marker than BDA we also injected an adeno.associated virus that encodes a fusion of channelrhodopsin-2 with the fluorescent protein Venus into the CAmy. ChR2-Venus containing fibers were present in the LC and Peri-LC zone with a pattern similar to that from BDA labeling (Figure 13). Many of the ChR2-Venus containing fibers were colocalized with GAD65/67-ir (Figure 13 C to F) and number of points of triple localization, Venus + GAD65/67-ir + TH-ir, could be identified (Figure 13 G to K). Because the results were qualitatively similar to those from BDA labeling we did not inject enough animals for quantitation of colocalizations.

To examine the possible direct connection of amygdalar and hypothalamic GABAergic axonal terminals with LC noradrenergic neurons we performed transneuronal anterograde tracing experiments. The H129 strain of HSV1 travels between neurons in an exclusively anterograde direction (Sun et al., 1996; Garner and LaVail, 1999; Szpara et al., 2010). David Anderson's group recently modified this virus so that it expresses the red fluorescent protein tdTomato following activation by Cre recombinase (Lo and Anderson, 2011). We injected this modified virus, HSV1-H129-LStdT, into the CAmy and PLH of VGAT-iCre/LSGFP mice in which GABAergic neurons express Cre recombinase and contain GFP (Figure 14). The spread of virus derived tdTomato was determined after 24, 48 and 72 hours for CAmy injections and 48 and 72 hours for PLH injections. A few tdTomato labeled cells were visible at the amygdalar injection site at 24 hours. Only one other very small group of labeled neurons, in the ipsilateral suprachiasmatic nucleus, was detected at this time anywhere in the brain. The number and the distribution of labeled neurons increased by 48 hours post injection, where in addition to the suprachiasmatic nucleus, tdTomato expressing neurons were found in the median preoptic nucleus, medial preoptic area, bed nucleus of the stria terminalis, lateral hypothalamus, arcuate nucleus, subparafascicular thalamic nucleus and periaqueductal gray. The labeling was almost exclusively on the injected side of the brain. There was no tdTomato in the LC area 24 and 48 hours post injection. tdTomato appeared in the LC 72 hours after HSV1-H129-LStdT injection into the CAmy (Figure 14 C

and D). LC neurons throughout the nucleus contained the viral marker in their soma and fibers. Many TH-ir neurons were labeled with tdTomato. Viral labeling was also observed in the contralateral LC as well as in non.adrenergic cells of the ipsilateral medial parabrachial nucleus (Figure 14E and F). The tracer did not label GABAergic neurons, identified by GFP expression in these VGAT-iCre/LSGFP mice, in the Peri-LC dendritic zone (Figure 14 E and F; G to J) or in the area closely adjacent to the LC (Figure 15). The very caudal part of the LC contralateral to the injection was also unlabeled at the 72 hour time point and no labeling was observed in regions caudal to the LC at this last time point.

Injection of HSV1-H129-LStdT into the PLH of VGAT-iCre/LSGFP mice labeled neurons at the injection site and in the zona incerta, dorsomedial hypothalamic, ventromedial hypothalamic and a few in the arcuate nucleus at 48 hours, but did not label the LC at this time point. A few labeled neurons were found in the median preoptic nucleus, medial preoptic area, around the PVN, and in the bed nucleus of the stria terminalis, periaqueductal gray and dorsal raphe nucleus at 72 hours. The LC nuclei bilaterally and the ipsilateral CAmy contained the greatest amount of tracer labeling 72 hours post injection. The pattern of LC labeling after PLH injection (Figure 16) was different from the CAmy injection. tdTomato was present both in LC TH-ir neurons (Figure 16 C to F) and also in GABAergic neurons in distal parts of the medial Peri-LC dendritic zone (Figure 16 G to J). The medial parabrachial nucleus did not contain label after this injection. Similar to CAmy injection, GABAergic neurons that closely surround the LC were also unlabeled (Figure 16 C to F) and the LC was the most caudal labeled nucleus after 72 hours.

A control injection of HSV1-H129-LStdT into the lateral part of the ventral posteromedial thalamic nucleus of a VGAT-iCre/LSGFP mouse labeled multiple cells that were exclusively in thalamic nuclei ipsilateral to the injection site. Not a single labeled neuron was found outside the thalamus 72 hours after the injection.

Discussion

Using mice that express GFP in GABAergic neurons we identified major GABAergic projections from the CAmy and PLH to the LC and the adjacent Peri-LC dendritic zone. The large number of GABAergic projection neurons from these regions is in striking contrast with lack of GABAergic innervation from the other forebrain areas that provide input to the LC such as the hypothalamic PVN and cerebral cortex. Using the conventional tracer BDA and adeno-associated virus expressing ChR2-Venus we observed that GABAergic fibers originating in the CAmy reached the LC and possibly made contact with TH dendrites in the surrounding dendritic zone throughout rostrocaudal extent of the LC, as well as within the Peri-LC dendritic zone. Direct connection of GABAergic projection neurons with noradrenergic LC neurons was strongly supported by results from infection of these cells following injection of the anterograde transneuronal tracer HSV1-H129-LStdT into the CAmy and PLH. This tracer labeled LC noradrenergic neurons but not GABAergic interneurons or non-GABAergic neurons in the Peri-LC zone.

Technical considerations

Proper injection placement is critical in anatomical tracing studies. More then one-third of the LC injected animals were excluded because the injection sites were outside the anatomical borders of the target nucleus. Even among the cases with properly positioned injections, with the end of the pipette track within the LC proper, a halo of FG extended medially into parts of the Barrington nucleus and laterally into the mesencephalic nucleus of the trigeminal nerve. The Peri-LC dendritic zone, which receives the majority of LC efferents merges into or overlaps with parts of the Barrington, medial parabrachial, and the mesencephalic trigeminal nucleus (Shipley et al., 1996) so we cannot completely exclude the possibility that some of the retrogradely labeled neurons actually innervate cells in these adjacent regions. However, the only part of the Barrington nucleus that contained labeled fibers following anterograde tracer injection into the CAmy was the region of potential overlap with the Peri-LC dendritic zone, suggesting that the majority of cells identified by retrograde tracer injection target LC neurons. Consistent with our observations, anterograde tracer injections into the CAmy and lateral hypothalamus performed by the Allen Brain Project produced patterns of LC area labeling identical to ours (available online http://www.brain.map.org/, section “Mouse Connectivity”, experiment 120281646 and experiment 11732771).

A second technical consideration is the validity of GFP expression by GAD67 synthesizing GABAergic neurons. Several previous studies have documented the GABAergic features of the GFP expressing neurons in the mouse line used (Brown et al., 2008; Suzuki and Bekkers, 2010; Wang and Bradley, 2010). GFP colocalized with several markers of GABA neurons including GAD67, calretinin, parvalbumin and somatostatin (Tamamaki et al., 2003). We confirmed some of these findings for the mice we used by double immunolabeling for GFP and calbindin and neuropeptide Y. Almost all calbindin.ir and neuropeptide Y-ir neurons in the amygdala coexpressed GFP-ir (data not shown). Also, puncta with GAD65/67-ir matched well with GFP-ir fibers after immunolabeling of hypothalamic and pontine sections (data not shown).

Our estimate that 30-40% of CAmy and PLH neurons that project to the LC are GABAergic is subject to several caveats. First, it is possible that not all GABAergic neurons express GAD67. Definitive studies evaluating the extent to which GABAergic neurons express both GAD65 and GAD67 have not been reported, and the identification of retrogradely labeled GABAergic neurons in this study relies on a marker driven by the GAD67 promoter, so it is possible that some GABA neurons were not visualized. However to our knowledge the only significant neuronal populations demonstrated to contain GAD65 and not GAD67 are the juxtaglomerlular cells in the olfactory bulb (Kiyokage et al., 2010), and in some areas complete overlap is documented (Esclapez et al., 1993). Also, the number and pattern of GFP containing cells in the amygdala appeared to be the same in the GAD67-GFP and VGAT-iCre/LSGFP mice (not shown). Second, estimates of the fraction of projection cells that are GABAergic are valid to the extent that different classes of projection neurons take up FG equally. It is worth noting that in one set of previous studies using cholera toxin B subunit for retrograde labeling in rat a CAmy projection to the LC area was not observed (Luppi et al., 1995). We speculate that this reflects selectivity in the neurons that take up or

transport cholera toxin under the conditions used, although we cannot exclude species differences or limited spread of the cholera toxin to the Peri-LC dendritic zone. It is not possible to extrapolate to the total number of NeuN-ir, GABAergic, or projection neurons in the CAmy because of the stringent criteria we used for selecting cells, incomplete labeling of projection cells by the tracer, and sampling at only three levels along the rostro-caudal axis which does not address the complex shape of the nucleus and potential variation in properties along this axis. However, based on the neurons observed it appears that at least several hundred neurons project from the CAmy and PLH to the LC. It seems likely that some of the GAD67-GFP negative neurons projecting from the CAmy to the LC use other transmitters that have been identified in the CAmy, including coricotropin releasing hormone, somatostatin, neurotensin and substance P (Moga and Gray, 1985; Shimada et al., 1989).

Sensory cortex projections to LC

Retrograde labeling of a small but well-defined group of non-GABAergic cells in the sensory cortex was unexpected. However, these sensory cortex projection neurons were found in all animals with proper injection sites. Projections from the medial prefrontal cortex to the LC are well described in rat (Luppi et al., 1995; Lu et al., 2012) and the study by Luppi et al also mentions labeled neurons in the somatosensory cortex corresponding to the lower limb. The Allen Brain Project has performed a series of anterograde tracer injections and made the images available via their website (http://connectivity.brain-map.org/). BDA injection into the somatosensory cortex of the trunk (case 10014655 and case 100141495) and lower limb (case 114292355 and case 112229814) of C57 mice labels projection fibers in the LC dendritic zone with occasional fibers in the LC proper. BDA injections into the somatosensory cortex of the mouth (case 112936582) and barrel field (112882565) showed very few but still clearly visible fibers reaching LC area. While the possibility that the FG labels fibers of passage cannot be completely excluded the observation that the anterogradely labeled fibers in this region do not travel much further caudally than the LC is consistent with them terminating there. The function of these projections and whether they are significant in other species remains to be determined.

Connection of GABAergic projection neurons to LC principal neurons

Our BDA and ChR2-Venus experiments do not explicitly address whether GABAergic projections from the CAmy, anterior hypothalamus and PLH make synaptic contacts with LC TH dendrites, since the defining morphological features of synapses are below light microscope resolution. We show that fibers that arise in the CAmy and PLH in which BDA is with colocalized GAD65/67-ir, or GFP in GAD67-GFP knock-in mice, are abundant in the LC and Peri-LC dendritic zone. Fibers that contain BDA or ChR2-Venus and GAD65/67-ir appear, at the limit of light microscope resolution, to contact TH-ir processes, which is consistent with the possibility of GABAergic projections from the CAmy synapsing with LC TH neurons. Support for synaptic connection was provided by HSV1-H129-LStdT labeling of LC neurons. HSV-H129 is documented to transfer from one neuron to another in a strictly anterograde direction (Sun et al., 1996; Garner and LaVail, 1999; Szpara et al., 2010). The tdTomato marker requires activation by Cre recombinase (Lo and Anderson, 2011) so red fluorescence appears in infected Cre expressing neurons or cells that

are infected from the Cre expressing neurons. While the virus can spread through multiple connected neurons, the time of LC labeling after the injections supports direct labeling of LC principal neurons from CAmy GABAergic neurons. Most other labeled forebrain areas were more distant form LC than the injection sites in the CAmy and PLH. Only the periaqueductal gray and dorsal raphe were closer to the LC but even at the 72 hour time point these two nuclei contained only very few scattered labeled neurons, far fewer than the large labeled population of the LC and surrounding area. It is unlikely that virus from CAmy injections reached the LC via the PLH because PLH injection resulted in a different labeling pattern and required 72 hours to label the LC. Interestingly, a viral injection into PLH labels the LC bilaterally and the ipsilateral CAmy after 72 hours, which would be possible only if the LC and CAmy were at similar axonal distances from PLH. Since there is a GABAergic projection from the CAmy to the LC with terminals that are adjacent to dendrites of TH-ir neurons, and TH-ir but not GABAergic cell bodies in the LC area contain the viral label, the data strongly support direct connection between CAmy GABAergic projection neurons and LC principal cells. Direct connection between PLH GABAergic and LC noradrenergic neurons also seems likely, because many more TH-ir neurons than GABAergic neurons contain label and the small number of labeled GABAergic neurons are in the most distal part of the Peri-LC dendritic zone, but a small amount of transfer between the populations cannot be completely excluded.

CAmy and bed nucleus of the stria terminalis projections to the LC that form inhibitory synapses with TH dendrites, based on a characteristic asymmetric structure observed by electron microscopy, have been described in rat but the nature of their transmitter was not established (Van Bockstaele et al., 1996; Van Bockstaele et al., 1999). GABAergic projections from ventrolateral preoptic nucleus to LC also have been suggested (Sherin et al., 1998; Lu et al., 2008) which is consistent with the FG/GAD67-GFP positive neurons in the same area observed in this study. A strong inhibitory input to TH dendrites that includes GABA and enkephalin as transmitters has been described, part of which originates in the brainstem (Van Bockstaele, 1998), but the origins of other parts have not been established. It seems likely that some of the BDA/GAD65/67-ir and BDA/GFP fibers documented here are a part of an inhibitory pathway to the LC that originates as FG/GAD67-GFP-ir neurons in the PLH and CAmy. The HSV1-H129-LStdT labeling of the LC proper but not of the GABA neurons in the adjacent Peri-LC area shows that the noradrenergic LC neurons are likely a direct target of these forebrain GABAergic projections. It is important to note that the cellular targets of neurons in other regions labeled by LC injected FG is not established and could be any of the neurons with cell bodies or dendrites in the area.

Another observation made in this study is that FG injections into LC retrogradely labeled many more cells in the CAmy, PVN and anterior hypothalamic nuclei on the injection side while anterograde labeling with HSV1-H129-LStdT injected into the CAmy produced labeling in the LC bilaterally. This suggests that there may be a small projection from the CAmy to the contralateral LC which becomes obvious using this method because even a very small amount of virus transfer produces a strong signal as the virus rapidly replicates. We found light contralateral LC labeling in cases of BDA CAmy injection, consistent with a small bilateral projection (not shown). These observations illustrate the sensitivity of circuit

tracing with a replicative virus but also show that caution must be used when interpreting the results quantitatively.

Functional implications of forebrain GABAergic projections

Amygdalar functions include coordination of emotional responses to stressful stimuli and part of this coordination is funneled through effects of the amygdala on the LC. Excitatory corticotrophin releasing factor projections from the CAmy to the Peri-LC dendritic zone have been described in rat (Van Bockstaele et al., 1996; Reyes et al., 2011). An inhibitory enkephalin signal arriving from the brainstem is also described (Van Bockstaele, 1998). These opposing influences very likely shape the active and passive coping behavior typical in stress responses. Another neuropeptide, neuropeptide-Y, exerts its anxiolytic activity via CAmy GABA neurons, some of which have been suggested to project to the LC (Tasan et al., 2010). Based on the large number of GABA neurons in the CAmy (Poulin et al., 2008), the presence of asymmetric, presumably inhibitory, synapses of amygdalar projection fibers on TH dendrites (Van Bockstaele et al., 1996) and the fact that some functional effects of amygdalar neurons require an inhibitory pathway to the brainstem, the existence of GABAergic projections from the CAmy to the LC has been accepted for some time (Swanson and Petrovich, 1998; Tasan et al., 2010). Our retrograde and anterograde experiments and use of GAD67-GFP expressing transgenic mice authenticate this putative inhibitory pathway in mice.

Multiple studies describe LC neurons as a central part of sleep-wake cycle circuitry. The neurons are excited during the wake state and are inhibited during sleep (Gompf and Aston-Jones, 2008). The existence of GABAergic neurons in the PLH that project to the LC has been suggested by studies of sleep but their existence was not structurally established (Verret et al., 2006; Hassani et al., 2010). Excitatory orexin and inhibitory melanin concentrating hormone neurons in the PLH exert their sleep-wake modulatory function, at least in part, by regulation of LC activity (Horvath et al., 1999). Some of the PLH melanin concentrating hormone neurons use GABA as a cotransmitter (Meister, 2007). Ventrolateral preoptic nucleus inhibitory input to LC has been established as a major factor for LC inhibition during sleep and loss of consciousness during anesthesia (Steininger et al., 2001; Gaus et al., 2002; Lu et al., 2008). A number of the GABAergic projection neurons described here may belong to this sleep-wake circuitry and inhibit the LC during sleep.

Modulation of LC effects on autonomic functions, conveyed by a robust efferent connection from the PVN is well established. Corticotrophin releasing factor is a transmitter in this projection (Valentino et al., 1992; Reyes et al., 2005) and corticotrophin releasing factor/glutamate terminals synapsing with TH dendrites have been demonstrated by electron microscopy (Valentino et al., 2001). Only 2% of the projections from the PVN to LC were found to contain the inhibitory neurotransmitter enkephalin (Reyes et al., 2005). These studies in rat are complemented by our findings in mouse, where the vast majority of PVN neurons that innervate the LC were GAD67-GFP negative and only a few isolated PVN projection neurons were GAD67-GFP positive. This suggests that in mouse, as in rat, the PVN output to LC is mostly excitatory. A potentially significant difference between rat and mouse is that we observed almost exclusively unilateral projections from the PVN to LC in

mouse, while in rat both sides project from the PVN to LC with very little difference between the ipsilateral and contralateral sides (Aston-Jones, 2004). Further studies will be required to determine whether these are strain-dependent, sex-dependant or species-dependent phenomena. We observed that all of the CAmy subnuclei project to the LC area, which is consistent with tract tracing studies in rat that show both centromedial (Veening et al., 1984) and centrolateral (Petrovich and Swanson, 1997) projections to the brainstem, although projections from the centromedial amygdala are described as more robust (Veening et al., 1984) and are emphasized in most recent literature (e.g. (Tasan et al., 2010)). Brainstem projections of both centrolateral and centromedial amygdalar GABAergic neurons are also described in nonhuman primate (Jongen-Relo and Amaral, 1998). In rat anterograde tracing showed centrolateral amygdalar projections to the medial parabrachial nucleus but not the LC (Petrovich and Swanson, 1997). Our data in mouse would be consistent with this if the retrograde labeling we observed in the centrolateral amygdala came from the Peri-LC region that overlaps with processes of medial parabrachial nucleus neurons, and the anterograde viral labeling in the medial parabrachial nucleus derived from virus spread into the centrolateral nucleus. This projection does appear to be strictly unilateral.

Our data shows that an inhibitory projection pathway containing the classic transmitter GABA directly connects parts of the amygdala and hypothalamus with the LC area. This is significant because it provides the structural basis for direct inhibitory modulation of noradrenergic LC neurons by forebrain structures. Very likely these inhibitory projections are part of the regulatory mechanisms for the sleep/wake cycle, stress responses, and other central autonomic functions in which the LC plays a central role. The transgenic mice characterized in this anatomical study are ideally suited for studies investigating the control of locus coeruleus function.

Acknowledgments

We appreciate the support provided by Milan Rusnak and Jonathan Kuo, the generous donation of Vgat$^{ires\text{-}Cre/+v}$ mice by Linh Vong and Bradford Lowell, RCE:LoxP mice by Gord Fishell, and HSV1-H129-LStdT virus by Liching Lo and David Anderson.

Support provided by the Intramural Program of the National Institute of Mental Health, ZIA MH002685-16

Role of authors: All authors had full access to all the data in the study and take responsibility for the integrity of the data and the accuracy of the data analysis. Study concept and design: ELD and TBU. Acquisition of data: ELD. Analysis and interpretation of data: ELD and TBU. Drafting of the manuscript: ELD and TBU. Development of critical reagents: YY. Critical revision of the manuscript for important intellectual content: ELD, YY, TBU.

Literature cited

Abercrombie M. Estimation of nuclear population from microtome sections. The Anatomical Record. 1946; 94:239–247. [PubMed: 21015608]

Allen, P. Allen Mouse Brain Atlas. Allen Institute for Brain Science; 2009.

Aston-Jones, G. Locus Coeruleus, A5 and A7 Noradrenergic Cell Groups.. In: Paxinos, G., editor. The Rat Nevous System. Third Edition Edition. Academic Press; San Diego, CA: 2004.

Aston-Jones G, Bloom FE. Activity of norepinephrine-containing locus coeruleus neurons in behaving rats anticipates fluctuations in the sleep-waking cycle. J Neurosci. 1981; 1:876–886. [PubMed: 7346592]

Aston-Jones G, Cohen JD. An integrative theory of locus coeruleus-norepinephrine function: adaptive gain and optimal performance. Annual review of neuroscience. 2005; 28:403–450.

Aston-Jones G, Zhu Y, Card JP. Numerous GABAergic afferents to locus ceruleus in the pericerulear dendritic zone: possible interneuronal pool. J Neurosci. 2004; 24:2313–2321. [PubMed: 14999082]

Aston-Jones G, Ennis M, Pieribone VA, Nickell WT, Shipley MT. The brain nucleus locus coeruleus: restricted afferent control of a broad efferent network. Science. 1986; 234:734–737. [PubMed: 3775363]

Aston-Jones G, Shipley MT, Chouvet G, Ennis M, van Bockstaele E, Pieribone V, Shiekhattar R, Akaoka H, Drolet G, Astier B, et al. Afferent regulation of locus coeruleus neurons: anatomy, physiology and pharmacology. Progress in brain research. 1991; 88:47–75. [PubMed: 1687622]

Barlow AL, Macleod A, Noppen S, Sanderson J, Guerin CJ. Colocalization analysis in fluorescence micrographs: verification of a more accurate calculation of pearson's correlation coefficient. Microsc Microanal. 2010; 16:710–724. [PubMed: 20946701]

Berridge CW, Waterhouse BD. The locus coeruleus-noradrenergic system: modulation of behavioral state and state-dependent cognitive processes. Brain research Brain research reviews. 2003; 42:33–84. [PubMed: 12668290]

Brown RE, McKenna JT, Winston S, Basheer R, Yanagawa Y, Thakkar MM, McCarley RW. Characterization of GABAergic neurons in rapid-eye-movement sleep controlling regions of the brainstem reticular formation in GAD67-green fluorescent protein knock-in mice. The European journal of neuroscience. 2008; 27:352–363. [PubMed: 18215233]

Cedarbaum JM, Aghajanian GK. Afferent projections to the rat locus coeruleus as determined by a retrograde tracing technique. J Comp Neurol. 1978; 178:1–16. [PubMed: 632368]

Dahlstroem A, Fuxe K, Olson L, Ungerstedt U. Ascending Systems of Catecholamine Neurons from the Lower Brain Stem. Acta physiologica Scandinavica. 1964; 62:485–486. [PubMed: 14252583]

Del Cid-Pellitero E, Garzon M. Hypocretin1/OrexinA-containing axons innervate locus coeruleus neurons that project to the Rat medial prefrontal cortex. Implication in the sleep-wakefulness cycle and cortical activation. Synapse. 2011; 65:843–857. [PubMed: 21308795]

Esclapez M, Tillakaratne NJ, Tobin AJ, Houser CR. Comparative localization of mRNAs encoding two forms of glutamic acid decarboxylase with nonradioactive in situ hybridization methods. J Comp Neurol. 1993; 331:339–362. [PubMed: 8514913]

Fallon JH, Koziell DA, Moore RY. Catecholamine innervation of the basal forebrain. II. Amygdala, suprarhinal cortex and entorhinal cortex. J Comp Neurol. 1978; 180:509–532. [PubMed: 659673]

Franklin, KBJ.; Paxinos, G., editors. The mouse brain in stereotaxic coordinates. 3rd Edition. Academic Press; New York,NY: 2008.

Garner JA, LaVail JH. Differential anterograde transport of HSV type 1 viral strains in the murine optic pathway. Journal of neurovirology. 1999; 5:140–150. [PubMed: 10321978]

Gaus SE, Strecker RE, Tate BA, Parker RA, Saper CB. Ventrolateral preoptic nucleus contains sleep-active, galaninergic neurons in multiple mammalian species. Neuroscience. 2002; 115:285–294. [PubMed: 12401341]

Geerling JC, Shin JW, Chimenti PC, Loewy AD. Paraventricular hypothalamic nucleus: axonal projections to the brainstem. J Comp Neurol. 2010; 518:1460–1499. [PubMed: 20187136]

Gompf HS, Aston-Jones G. Role of orexin input in the diurnal rhythm of locus coeruleus impulse activity. Brain research. 2008; 1224:43–52. [PubMed: 18614159]

Gompf HS, Mathai C, Fuller PM, Wood DA, Pedersen NP, Saper CB, Lu J. Locus ceruleus and anterior cingulate cortex sustain wakefulness in a novel environment. J Neurosci. 2010; 30:14543–14551. [PubMed: 20980612]

Hassani OK, Henny P, Lee MG, Jones BE. GABAergic neurons intermingled with orexin and MCH neurons in the lateral hypothalamus discharge maximally during sleep. The European journal of neuroscience. 2010; 32:448–457. [PubMed: 20597977]

Hendreen JC. What was wrong with the Abercombie and Empirical cell counting methods? A review. The Anatomical Record. 1998; 250:373–380. [PubMed: 9517854]

Henny P, Brischoux F, Mainville L, Stroh T, Jones BE. Immunohistochemical evidence for synaptic release of glutamate from orexin terminals in the locus coeruleus. Neuroscience. 2010; 169:1150–1157. [PubMed: 20540992]

Hopkins DA, Holstege G. Amygdaloid projections to the mesencephalon, pons and medulla oblongata in the cat. Exp Brain Res. 1978; 32:529–547. [PubMed: 689127]

Hopman AH, Ramaekers FC, Speel EJ. Rapid synthesis of biotin-, digoxigenin-, trinitrophenyl-, and fluorochrome-labeled tyramides and their application for In situ hybridization using CARD amplification. J Histochem Cytochem. 1998; 46:771–777. [PubMed: 9603790]

Horvath TL, Peyron C, Diano S, Ivanov A, Aston-Jones G, Kilduff TS, van Den Pol AN. Hypocretin (orexin) activation and synaptic innervation of the locus coeruleus noradrenergic system. J Comp Neurol. 1999; 415:145–159. [PubMed: 10545156]

Jongen-Relo AL, Amaral DG. Evidence for a GABAergic projection from the central nucleus of the amygdala to the brainstem of the macaque monkey: a combined retrograde tracing and in situ hybridization study. The European journal of neuroscience. 1998; 10:2924–2933. [PubMed: 9758162]

Kiyokage E, Pan YZ, Shao Z, Kobayashi K, Szabo G, Yanagawa Y, Obata K, Okano H, Toida K, Puche AC, Shipley MT. Molecular identity of periglomerular and short axon cells. J Neurosci. 2010; 30:1185–1196. [PubMed: 20089927]

Lee HS, Kim MA, Waterhouse BD. Retrograde double-labeling study of common afferent projections to the dorsal raphe and the nuclear core of the locus coeruleus in the rat. J Comp Neurol. 2005; 481:179–193. [PubMed: 15562508]

Lo L, Anderson DJ. A Cre-dependent, anterograde transsynaptic viral tracer for mapping output pathways of genetically marked neurons. Neuron. 2011; 72:938–950. [PubMed: 22196330]

Lu J, Nelson LE, Franks N, Maze M, Chamberlin NL, Saper CB. Role of endogenous sleep-wake and analgesic systems in anesthesia. J Comp Neurol. 2008; 508:648–662. [PubMed: 18383504]

Lu Y, Simpson KL, Weaver KJ, Lin RC. Differential distribution patterns from medial prefrontal cortex and dorsal raphe to the locus coeruleus in rats. Anat Rec (Hoboken). 2012; 295:1192–1201. [PubMed: 22674904]

Luppi PH, Aston-Jones G, Akaoka H, Chouvet G, Jouvet M. Afferent projections to the rat locus coeruleus demonstrated by retrograde and anterograde tracing with cholera-toxin B subunit and Phaseolus vulgaris leucoagglutinin. Neuroscience. 1995; 65:119–160. [PubMed: 7753394]

Marowsky A, Yanagawa Y, Obata K, Vogt KE. A specialized subclass of interneurons mediates dopaminergic facilitation of amygdala function. Neuron. 2005; 48:1025–1037. [PubMed: 16364905]

Meister B. Neurotransmitters in key neurons of the hypothalamus that regulate feeding behavior and body weight. Physiology & behavior. 2007; 92:263–271. [PubMed: 17586536]

Miyawaki T, Kawamura H, Komatsu K, Yasugi T. Chemical stimulation of the locus coeruleus: inhibitory effects on hemodynamics and renal sympathetic nerve activity. Brain research. 1991; 568:101–108. [PubMed: 1687667]

Moga MM, Gray TS. Evidence for corticotropin-releasing factor, neurotensin, and somatostatin in the neural pathway from the central nucleus of the amygdala to the parabrachial nucleus. J Comp Neurol. 1985; 241:275–284. [PubMed: 2868027]

Petrovich GD, Swanson LW. Projections from the lateral part of the central amygdalar nucleus to the postulated fear conditioning circuit. Brain research. 1997; 763:247–254. [PubMed: 9296566]

Peyron C, Tighe DK, van den Pol AN, de Lecea L, Heller HC, Sutcliffe JG, Kilduff TS. Neurons containing hypocretin (orexin) project to multiple neuronal systems. J Neurosci. 1998; 18:9996–10015. [PubMed: 9822755]

Poulin JF, Castonguay-Lebel Z, Laforest S, Drolet G. Enkephalin co-expression with classic neurotransmitters in the amygdaloid complex of the rat. J Comp Neurol. 2008; 506:943–959. [PubMed: 18085591]

Price JL. Subcortical projections from the amygdaloid complex. Advances in experimental medicine and biology. 1986; 203:19–33. [PubMed: 3098058]

Price JL, Amaral DG. An autoradiographic study of the projections of the central nucleus of the monkey amygdala. J Neurosci. 1981; 1:1242–1259. [PubMed: 6171630]

Puskas N, Papp RS, Gallatz K, Palkovits M. Interactions between orexin-immunoreactive fibers and adrenaline or noradrenaline-expressing neurons of the lower brainstem in rats and mice. Peptides. 2010; 31:1589–1597. [PubMed: 20434498]

Reyes BA, Valentino RJ, Xu G, Van Bockstaele EJ. Hypothalamic projections to locus coeruleus neurons in rat brain. The European journal of neuroscience. 2005; 22:93–106. [PubMed: 16029199]

Reyes BA, Carvalho AF, Vakharia K, Van Bockstaele EJ. Amygdalar peptidergic circuits regulating noradrenergic locus coeruleus neurons: linking limbic and arousal centers. Experimental neurology. 2011; 230:96–105. [PubMed: 21515261]

Saper CB, Swanson LW, Cowan WM. The efferent connections of the ventromedial nucleus of the hypothalamus of the rat. J Comp Neurol. 1976; 169:409–442. [PubMed: 61975]

Saper CB, Swanson LW, Cowan WM. An autoradiographic study of the efferent connections of the lateral hypothalamic area in the rat. J Comp Neurol. 1979; 183:689–706. [PubMed: 105019]

Sherin JE, Elmquist JK, Torrealba F, Saper CB. Innervation of histaminergic tuberomammillary neurons by GABAergic and galaninergic neurons in the ventrolateral preoptic nucleus of the rat. J Neurosci. 1998; 18:4705–4721. [PubMed: 9614245]

Shimada S, Inagaki S, Kubota Y, Ogawa N, Shibasaki T, Takagi H. Coexistence of peptides (corticotropin releasing factor/neurotensin and substance P/somatostatin) in the bed nucleus of the stria terminalis and central amygdaloid nucleus of the rat. Neuroscience. 1989; 30:377–383. [PubMed: 2473417]

Shipley MT, Fu L, Ennis M, Liu WL, Aston-Jones G. Dendrites of locus coeruleus neurons extend preferentially into two pericoerulear zones. J Comp Neurol. 1996; 365:56–68. [PubMed: 8821441]

Sirieix C, Gervasoni D, Luppi PH, Leger L. Role of the lateral paragigantocellular nucleus in the network of paradoxical (REM) sleep: an electrophysiological and anatomical study in the rat. PLoS One. 2012; 7:e28724. [PubMed: 22235249]

Sousa VH, Miyoshi G, Hjerling-Leffler J, Karayannis T, Fishell G. Characterization of Nkx6-2-derived neocortical interneuron lineages. Cereb Cortex 19 Suppl. 2009; 1:i1–10.

Steininger TL, Gong H, McGinty D, Szymusiak R. Subregional organization of preoptic area/anterior hypothalamic projections to arousal-related monoaminergic cell groups. J Comp Neurol. 2001; 429:638–653. [PubMed: 11135241]

Sun N, Cassell MD, Perlman S. Anterograde, transneuronal transport of herpes simplex virus type 1 strain H129 in the murine visual system. Journal of virology. 1996; 70:5405–5413. [PubMed: 8764051]

Suzuki N, Bekkers JM. Inhibitory neurons in the anterior piriform cortex of the mouse: classification using molecular markers. J Comp Neurol. 2010; 518:1670–1687. [PubMed: 20235162]

Sved AF, Felsten G. Stimulation of the locus coeruleus decreases arterial pressure. Brain research. 1987; 414:119–132. [PubMed: 2887237]

Swanson SW, Petrovich GD. What is the amygdala. Trends Neurosci. 1998:323–331. [PubMed: 9720596]

Szpara ML, Parsons L, Enquist LW. Sequence variability in clinical and laboratory isolates of herpes simplex virus 1 reveals new mutations. Journal of virology. 2010; 84:5303–5313. [PubMed: 20219902]

Tamamaki N, Yanagawa Y, Tomioka R, Miyazaki J, Obata K, Kaneko T. Green fluorescent protein expression and colocalization with calretinin, parvalbumin, and somatostatin in the GAD67-GFP knock-in mouse. J Comp Neurol. 2003; 467:60–79. [PubMed: 14574680]

Tasan RO, Nguyen NK, Weger S, Sartori SB, Singewald N, Heilbronn R, Herzog H, Sperk G. The central and basolateral amygdala are critical sites of neuropeptide Y/Y2 receptor-mediated regulation of anxiety and depression. J Neurosci. 2010; 30:6282–6290. [PubMed: 20445054]

Valentino RJ, Page M, Van Bockstaele E, Aston-Jones G. Corticotropin-releasing factor innervation of the locus coeruleus region: distribution of fibers and sources of input. Neuroscience. 1992; 48:689–705. [PubMed: 1376457]

Valentino RJ, Rudoy C, Saunders A, Liu XB, Van Bockstaele EJ. Corticotropin-releasing factor is preferentially colocalized with excitatory rather than inhibitory amino acids in axon terminals in the peri-locus coeruleus region. Neuroscience. 2001; 106:375–384. [PubMed: 11566507]

Van Bockstaele EJ. Morphological substrates underlying opioid, epinephrine and gamma-aminobutyric acid inhibitory actions in the rat locus coeruleus. Brain research bulletin. 1998; 47:1–15. [PubMed: 9766384]

Van Bockstaele EJ, Chan J, Pickel VM. Input from central nucleus of the amygdala efferents to pericoerulear dendrites, some of which contain tyrosine hydroxylase immunoreactivity. Journal of neuroscience research. 1996; 45:289–302. [PubMed: 8841990]

Van Bockstaele EJ, Peoples J, Valentino RJ. A.E. Bennett Research Award. Anatomic basis for differential regulation of the rostrolateral peri-locus coeruleus region by limbic afferents. Biological psychiatry. 1999; 46:1352–1363. [PubMed: 10578450]

Van Bockstaele EJ, Bajic D, Proudfit H, Valentino RJ. Topographic architecture of stress-related pathways targeting the noradrenergic locus coeruleus. Physiology & behavior. 2001; 73:273–283. [PubMed: 11438352]

Veening JG, Swanson LW, Sawchenko PE. The organization of projections from the central nucleus of the amygdala to brainstem sites involved in central autonomic regulation: a combined retrograde transport-immunohistochemical study. Brain research. 1984; 303:337–357. [PubMed: 6204716]

Verret L, Fort P, Gervasoni D, Leger L, Luppi PH. Localization of the neurons active during paradoxical (REM) sleep and projecting to the locus coeruleus noradrenergic neurons in the rat. J Comp Neurol. 2006; 495:573–586. [PubMed: 16498678]

Vong L, Ye C, Yang Z, Choi B, Chua S Jr. Lowell BB. Leptin action on GABAergic neurons prevents obesity and reduces inhibitory tone to POMC neurons. Neuron. 2011; 71:142–154. [PubMed: 21745644]

Wallace DM, Magnuson DJ, Gray TS. The amygdalo-brainstem pathway: selective innervation of dopaminergic, noradrenergic and adrenergic cells in the rat. Neuroscience letters. 1989; 97:252–258. [PubMed: 2717061]

Wang M, Bradley RM. Properties of GABAergic neurons in the rostral solitary tract nucleus in mice. Journal of neurophysiology. 2010; 103:3205–3218. [PubMed: 20375246]

Wei F, Dubner R, Ren K. Nucleus reticularis gigantocellularis and nucleus raphe magnus in the brain stem exert opposite effects on behavioral hyperalgesia and spinal Fos protein expression after peripheral inflammation. Pain. 1999; 80:127–141. [PubMed: 10204725]

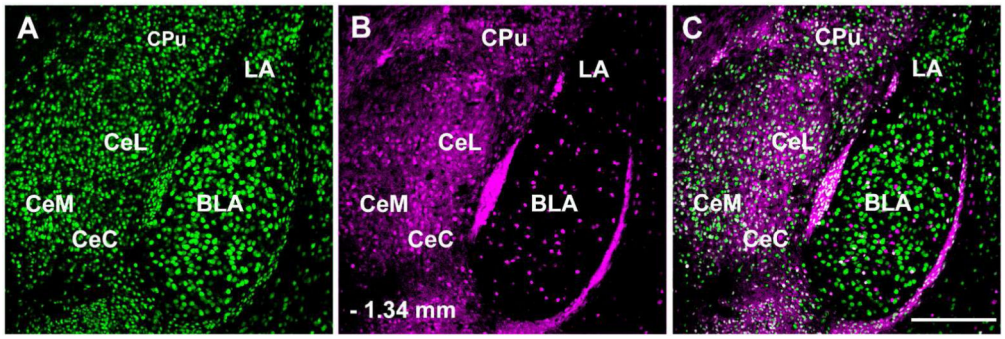

Figure 1.

Distribution of Green Fluorescent Protein (GFP) containing neurons in the amygdala of a GAD67-GFP knock-in mouse. NeuN-ir (A) labels the entire neuronal population. Large numbers of GFP-ir neurons (B) are present throughout the central amygdala, while much smaller numbers are seen in the basolateral amygdala, and lateral amygdala. Panel C contains a merged image. Abbreviations: BLA – basolateral amygdala, CeC – centrocentral, CeL – centrolateral amygdala, CeM – centromedial amygdala, CPu – caudate putamen, LA – lateral amygdala. – 1.46 mm to bregma. Scale bar = 200 μm.

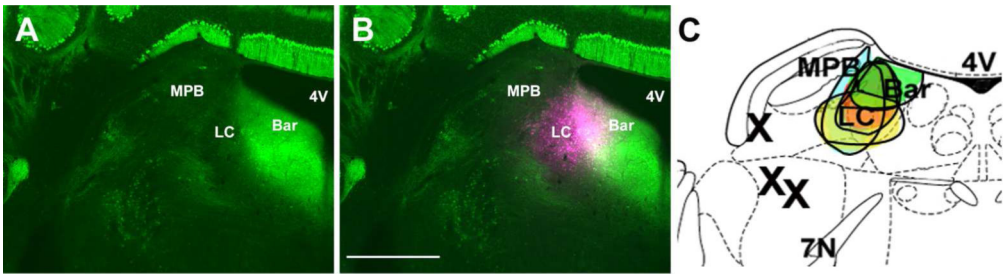

Figure 2.

Position of fluorogold (FG) injection sites in the locus coeruleus (LC). Panel A shows a coronal section through the dorsal pons with the LC and adjacent anatomical structures. The visible neurons and fibers are from native GFP fluorescence of the GAD67-GFP knock-in mouse. Panel B shows a FG injection site and the radius of tracer diffusion. Panel C is a schematic drawing from “The mouse brain in stereotaxic coordinates”, (K. Franklin at al., 2008) that shows the four injection sites in different shades from animals included in the analysis of LC afferents. The three Xs indicate the injection sites of animals that were excluded from analysis. Abbreviations: 4V – fourth ventricle, 7N – seventh cranial nerve, Bar – Barrington nucleus, LC – locus coeruleus and MPB – medial parabrachial nucleus. Scale bar = 500 μm.

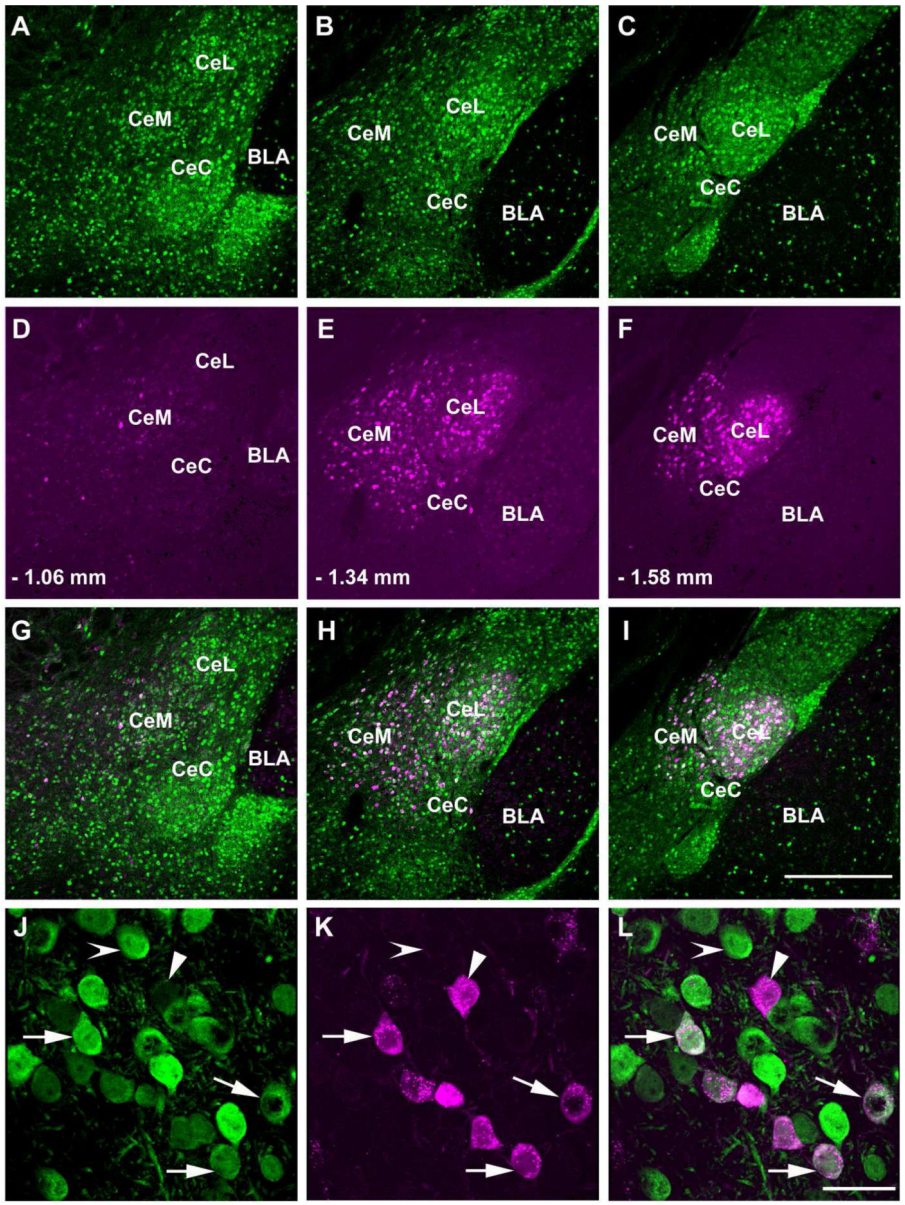

Figure 3.

Distribution of GAD67 expressing cells in the central amygdala (CAmy) that project to the LC. Panels A-C show GAD67-GFP-ir neurons at three coronal levels. Panel D-F (corresponding to the panels just above) show FG-ir labeled neurons in the CAmy after FG injection in the LC. Numbers indicate the distance from bregma. Panels G-I contain merged images of the two panels above them. The largest number of FG containing neurons and FG-ir neurons that colocalize with GAD67-GFP-ir is in the middle section of the CAmy (B, E and H) and the lowest number is in the anterior section (A, D and G). Panels J-L are high magnification images of LC injected FG in centromedial amygdalar GAD67-GFP-ir neurons. Arrows in panel J point to neurons in the centromedial amygdala that coexpress GAD67-GFP-ir and FG (panel K). An arrowhead points to a cell that contains only FG and an indented arrowhead to a neuron with only GAD67-GFP-ir. Panel L contains a merged

image. Abbreviations: BLA –basolateral amygdala, CeC - centrocentral amygdala, CeL – centrolateral amygdala, CeM – centromedial amygdala. Scale bar = 500 μm for A to I and scale bar = 20 μm for J to L.

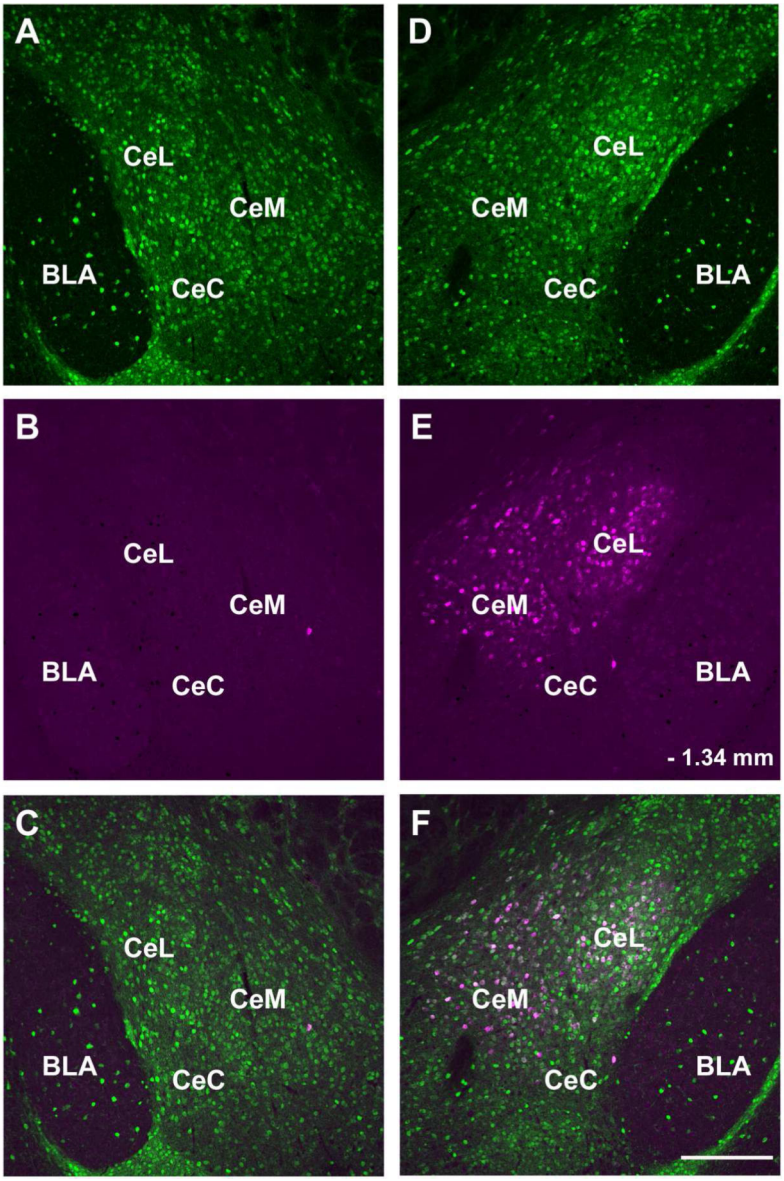

Figure 4.

The CAmy to LC projection is strictly ipsilateral. Panels A, B, and C show the right side and panels D, E and F the left side of a single coronal section from an animal injected with FG into the left LC. Only cells in the left CAmy contain significant FG signal. Panels A and D show GAD67-GFP-ir neurons, panels B and E show FG-ir cells. Panels C and F contain merged images. Abbreviations: BLA – basolateral amygdala, CeC – centrocentral amygdala, CeL – centrolateral amygdala, CeM – centromedial amygdala. – 1.34 mm indicates distance from bregma. Scale bar = 200 μm.

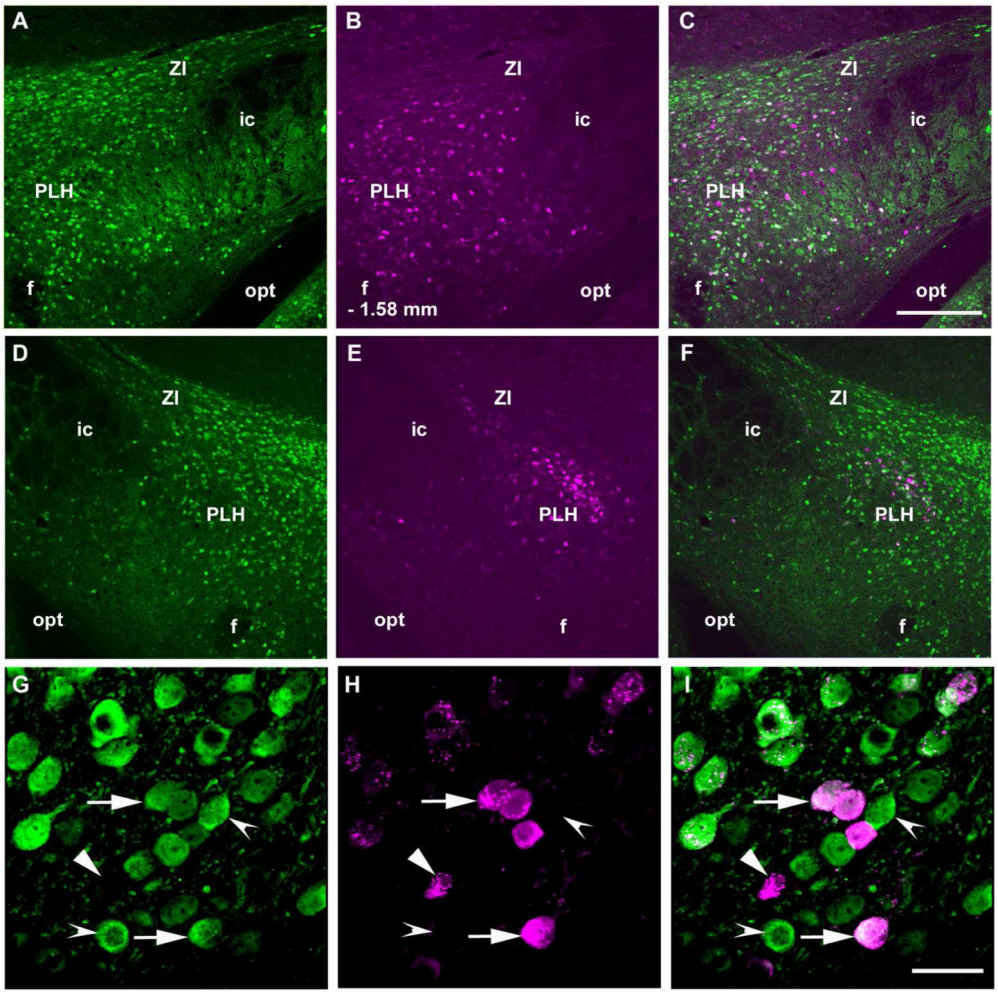

Figure 5.

Distribution of GAD67 expressing cells in the posterior lateral hypothalamus (PLH) that project to the LC. Panels A and D show GAD67-GFP-ir neurons and panels B and E show FG containing neurons. Panel C contains a merged image on the side ipsilateral to the FG injection with numerous neurons that contain both markers. A few double-labeled neurons can be seen in the merged image on the contralateral side (F). In higher magnification images from the ipsilateral side (G-I) colocalization of GAD67-GFP-ir (G) and FG-ir (H) can be more clearly seen. Arrows point to neurons that coexpress GAD67-GFP-ir and FG-ir. The arrowhead points to a cell that contains only FG and the indented arrowhead to a neuron with only GAD67-GFP-ir. Abbreviations: ic – internal capsule, f – fornix, opt – optic tract, PLH – posterior lateral hypothalamus, ZI – zona incerta. −1.58 indicates distance from bregma. Scale bar = 200 m for A to F and scale bar = 20 μm for G to L.

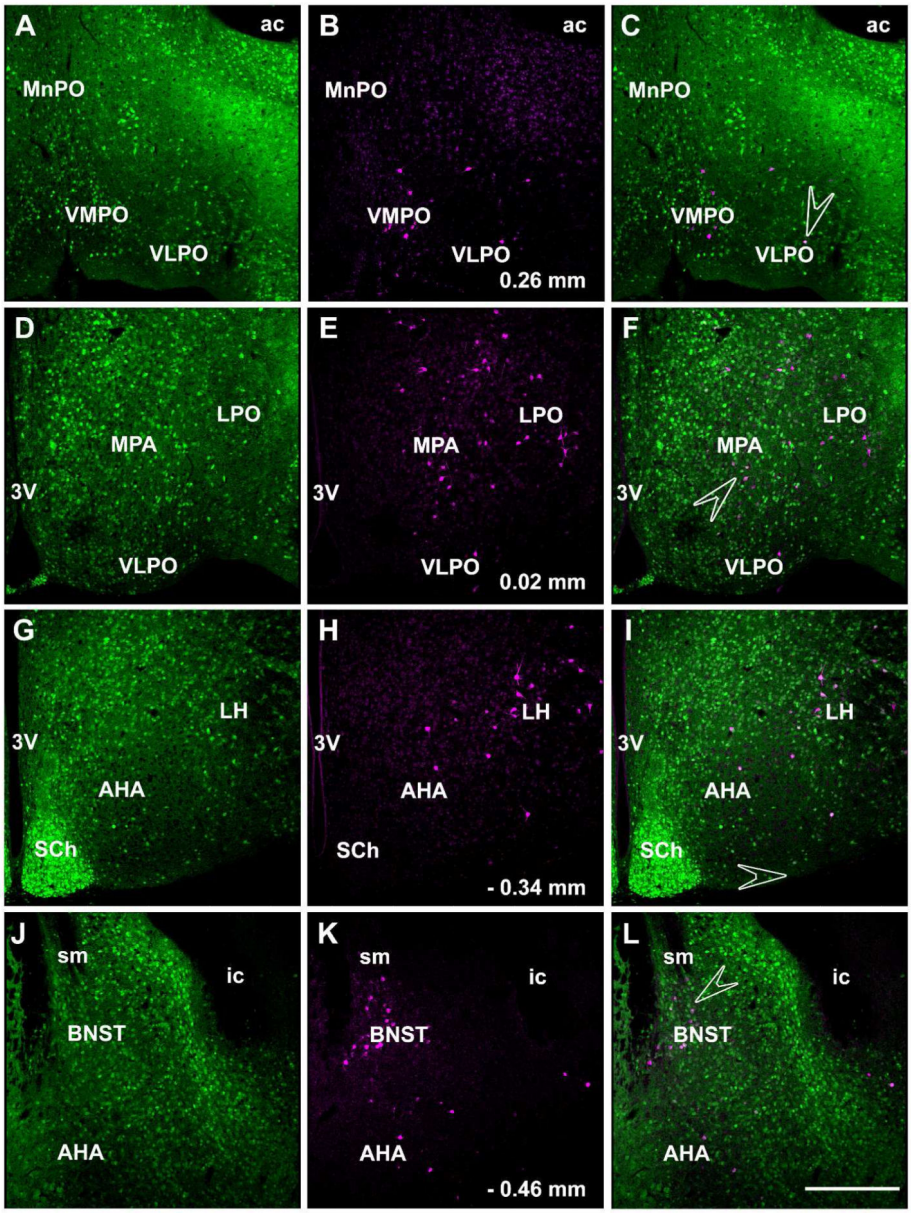

Figure 6.

Distribution of FG labeled cells in the anterior hypothalamic area after LC injection of FG. Panels in the left column show GAD67-GFP-ir neurons and panels in the middle column show FG containing neurons and the right column contains merged images. Many of the cells in the ventromedial and ventrolateral preoptic nuclei (A-C), medial and lateral preoptic areas (D-F), anterior hypothalamic area and lateral hypothalamus (G-I) and bed nucleus of stria terminalis (J-L) that are retrogradely labeled after FG injection into the LC contain GAD67-GFP-ir. Numbers indicated distance from bregma. Arrowheads point to the areas presented as high power images in figure 7. Abbreviations: 3V – third ventricle, ac – anterior commissura, AHA – anterior hypothalamic area, BNST – bed nucleus of stria terminalis, ic – internal capsule, LH – lateral hypothalamic area, LPO – lateral preoptic area, MPA – medial preoptic area, MnPO – median preoptic nucleus, SCh – suprachiasmatic

nucleus, sm – stria medularis, VLPO – ventrolateral preoptic nucleus, VMPO – ventromedial preoptic nucleus. Scale bar = 200 μm.

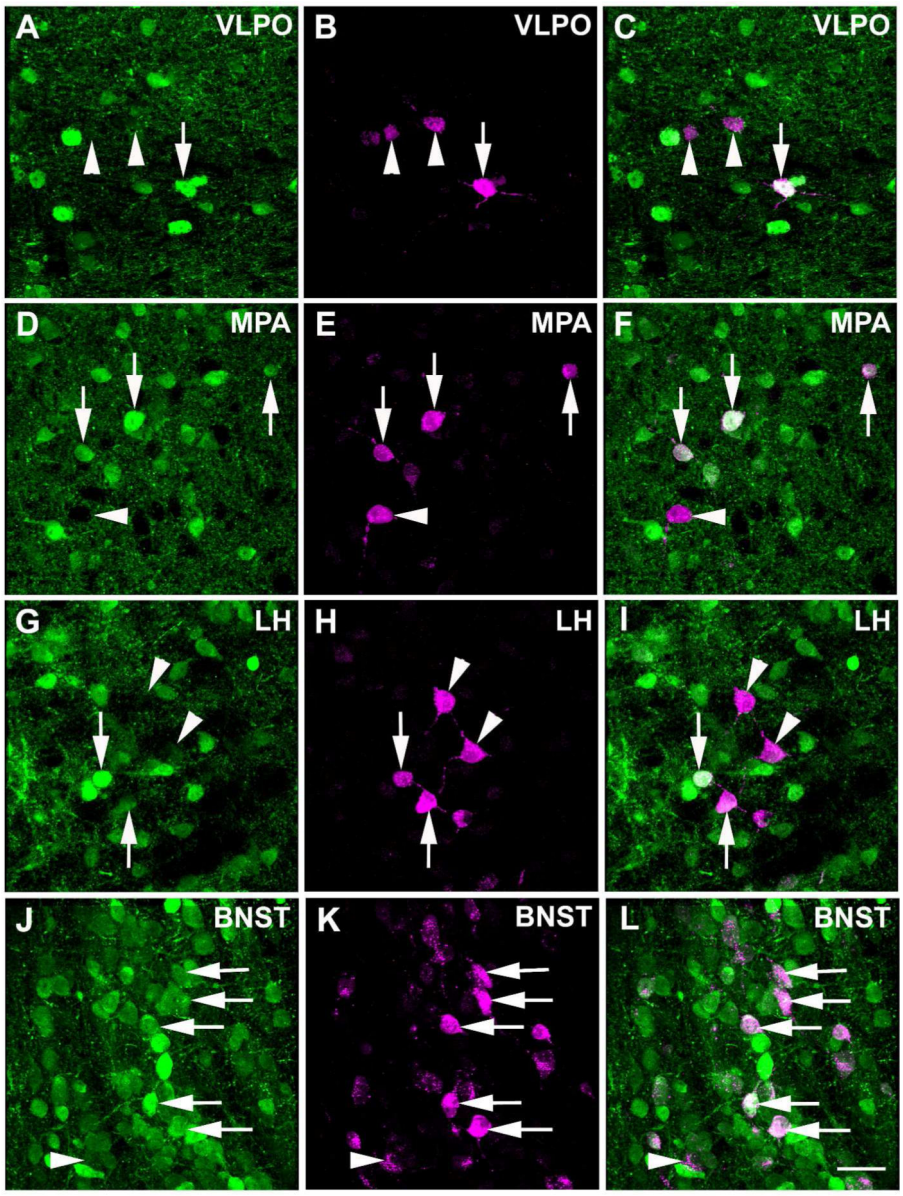

Figure 7.

High power images of the anterior hypothalamic areas presented in figure 6. Panels in the left column show GAD67-GFP-ir neurons, the middle panels show FG-ir and the right panels are merged images. The arrows point to a double-labeled cells. Arrowheads point to FG labeled cells in the same nuclei without visible colocalization of the GFP marker. Abbreviations: BNST – bed nucleus of stria terminalis, LH – lateral hypothalamus, MPA – medial preoptic area, VLPO – ventrolateral preoptic nucleus. Scale bar = 20 μm.

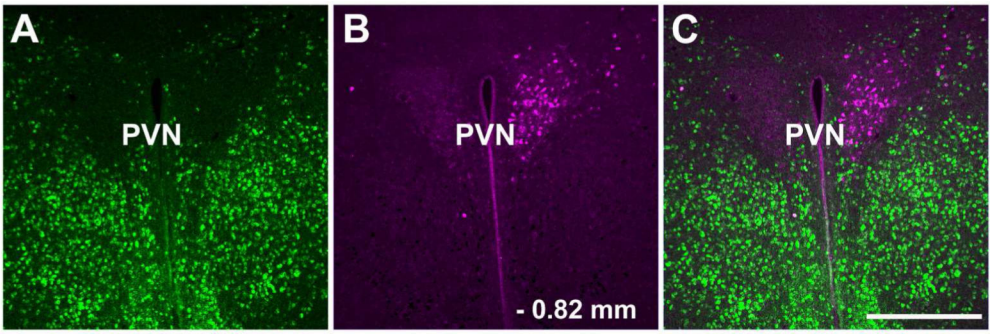

Figure 8.

Distribution of FG containing cells in the hypothalamic paraventricular nucleus after injection into LC. Panel A shows GAD67-GFP-ir neurons in the paraventricular nucleus and anterior hypothalamus, panel B shows FG labeled paraventricular neurons and panel C is a merged image. The retrogradely labeled cells in the paraventricular nucleus do not contain GAD67-GFP-ir. Scale bar = 200 μm. Abbreviations: PVN – paraventricular hypothalamic nucleus.

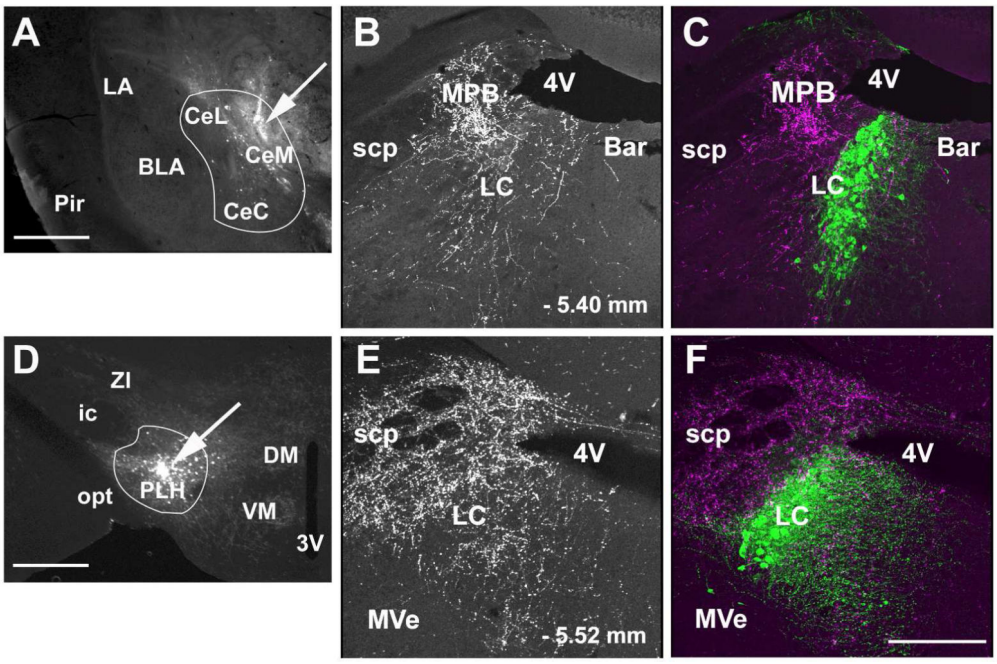

Figure 9.

Anterograde labeling in the LC following CAmy and PLH injection of BDA. Panel A shows a coronal section through the amygdala. An arrow points to a centromedial amygdalar injection site. A white line delineates the CAmy. In Panel D an arrow points to the site of a BDA injection into the PLH. A white line delineates the PLH. Anterogradely labeled fibers are shown in the dorsal pons after BDA injection into the CAmy (B and C) and PLH (E and F). The greatest fiber density is just lateral to the cluster of TH-ir LC neurons after both injections. Both also show a lower density of fibers traversing the LC proper and some fibers present in the rostromedial Peri-LC dendritic zone. Panels B and E show only labeling of the BDA containing fibers. Panels C and F show BDA labeling and TH-ir cells. Abbreviations: 3V – third ventricle, 4V – fourth ventricle, Bar – Barrington nucleus, BLA – basolateral amygdala, CeL – centrolateral amygdala, CeM – centromedial amygdala, CeC – centrocentral amygdala, DMH – dorsomedial hypothalamic nucleus, ic – internal capsule, LC – locus ceruleus, MPB – medial parabrachial nucleus, MVe – medial vestibular nucleus, opt – optic tract, Pir – piriform cortex, PLH – posterior lateral hypothalamus, scp – superior cerebellar pedunculus, SuVe – superior vestibular nucleus, VMH – ventromedial hypothalamic nucleus, ZI – zona incerta. – 1.34mm and – 1.58 mm indicate distance to bregma in A and D; – 5.40 mm and – 5.68 mm indicate distance to bregma in B, C, E and F. Scale bar = 500 μm for A and D and scale bar = 200 μm for B and C, E and F.

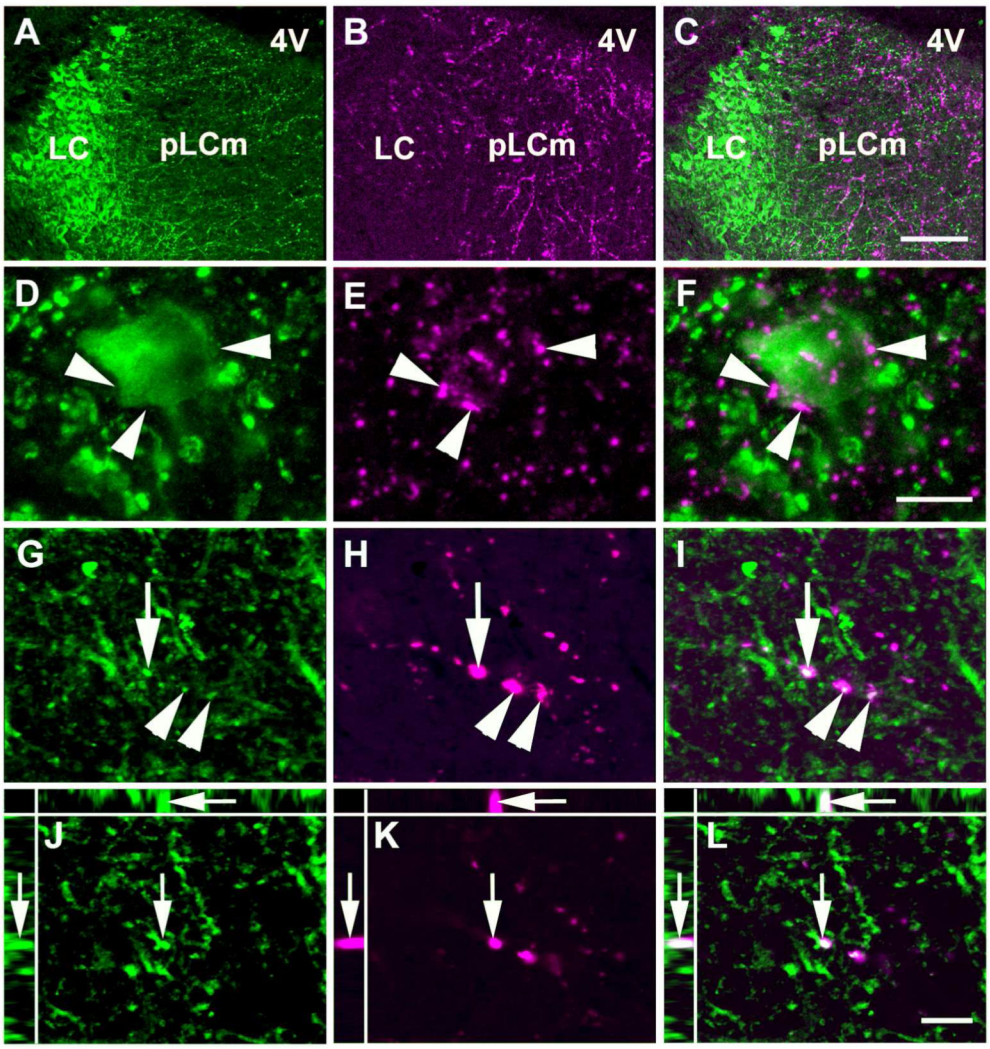

Figure 10.

LC distribution of BDA labeled neuronal fibers projecting from the CAmy. The fibers are densest in the LC dendritic zone, with fewer entering into the LC proper. The images are from the brain with a CeAm BDA injection shown in figure 9A. Panels in the left column show TH-ir, panels in the middle column show BDA labeling and the right column contains merged images. Panels A-C show the LC proper and the rostromedial Peri-LC dendritic zone. Panels D-F show a TH-ir neuron in the LC proper surrounded by BDA containing fibers. Panels G-I show TH-ir positive fibers in the dendritic zone and apparently colocalized BDA containing fibers. Panels J-L are a XYZ presentation (larger panel X-Y, with Y-Z left and X-Z top) of a single optical section from the confocal Z stack in G-I. Arrowheads indicate puncta with possible colocalization between TH-ir and BDA. The arrow points to a TH-ir/BDA puncta with apparent colocalization, that is also shown in the XYZ single optical section. Abbreviations: 4V – fourth ventricle, LC – locus coeruleus, pLCrm – rostromedial pericoerulear region. Scale bar = 100 μm in uppermost panels, 20 μm in the two middle panels and 5 μm in the lowest panels.

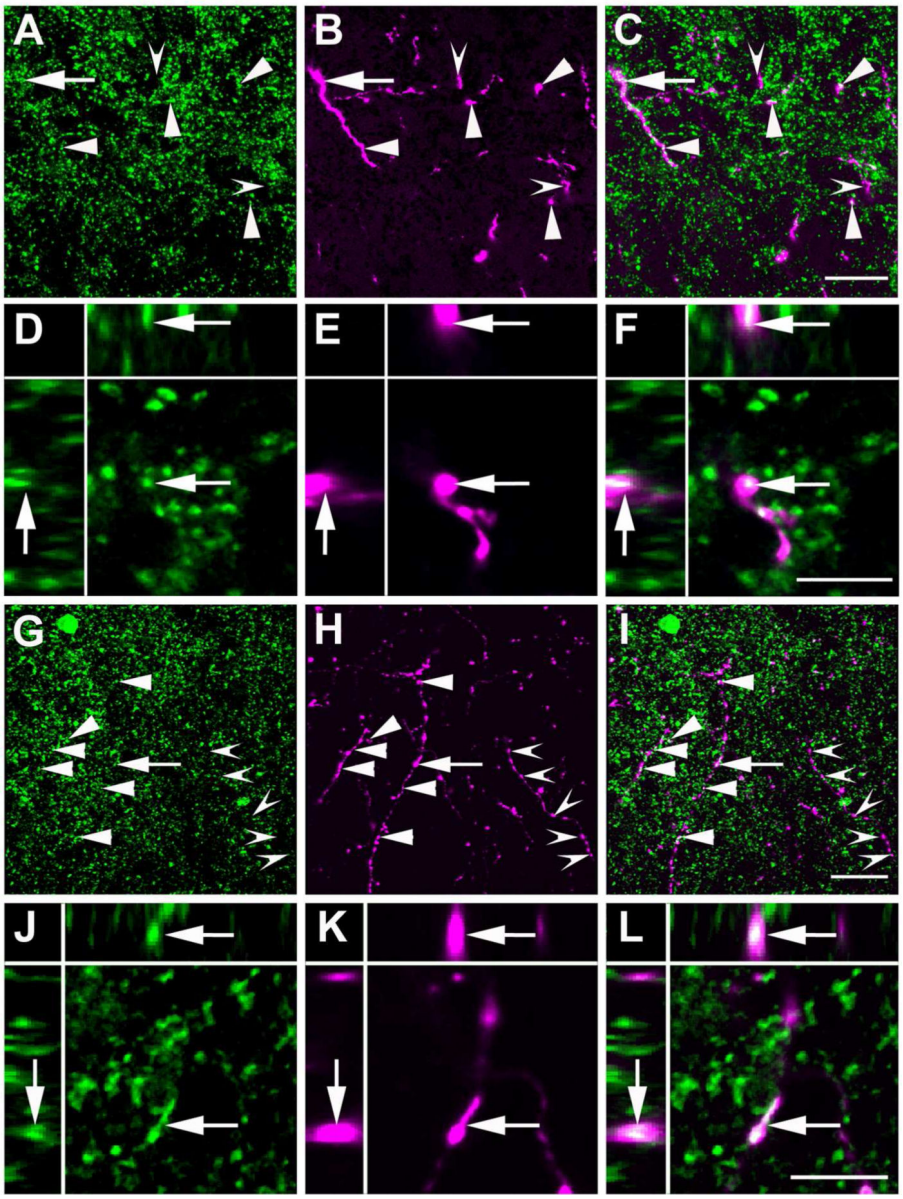

Figure 11.

BDA labeled neuronal fibers projecting from the CAmy into the LC dendritic zone contain GAD65/67-ir. Panels A to F are from a wild-type mouse after BDA injection into the centromedial amydala. Panels A (GAD65/67-ir), B (BDA) and C (merged image) contain a summed confocal Z stack of 10 optical sections collected with a step of 0.42 μm. Panels D-F are a XYZ presentation of a single optical section from the Z stack in A-C. Overlap of GAD65/67-ir and BDA appears white in the merged images in panels C and F. Arrowheads indicate areas with apparent colocalization of GAD65/67-ir and BDA and indented arrowheads point to puncta with only BDA labeling. The arrow points to a region of apparent GAD65/67-ir and BDA colocalization that is shown at higher magnification in single optical sections in the lower panels (larger panel X-Y, with Y-Z left and X-Z top). Panels G to L are from a GAD67-GFP knock-in mouse with a centromedial amygdalar BDA

injection. Panels G-I contain summed confocal Z stacks of 10 optical sections collected with a step of 0.42 μm. Panels J-L are a XYZ (larger panel X-Y, with Y-Z left and X-Z top) presentation of single optical sections from the Z stack in G-I. Panels G and J show GFP-ir and panels H and K show BDA labeling. Panels I and L contain merged images. Arrowheads indicate areas with possible colocalization of GFP-ir and BDA and indented arrowheads point to puncta with only BDA labeling. The arrow points to an area containing apparent GFP-ir and BDA co-labeling that is shown at higher magnification in single optical sections in the lower panels. Scale bar = 20 μm in panels A-C and G-I panels and = 5 μm in D-F and J-L.

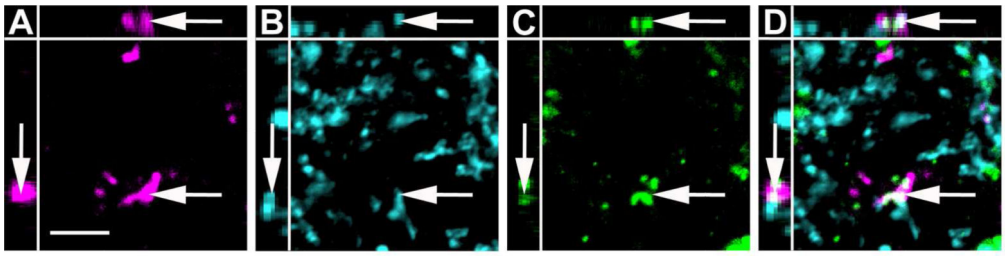

Figure 12.

High magnification image of anterogradely labeled CAmy fibers adjacent to TH-ir processes in the LC. An example of possible colocalization between BDA (A), GAD65/67-ir (B) and TH-ir (C) in the LC dendritic zone after injection of BDA in the CAmy is shown (arrow). Panel D contains a merged image. Images are single optical sections presented as a XYZ image (larger panel X-Y, with Y-Z left and X-Z top). Scale bar = 5 μm.

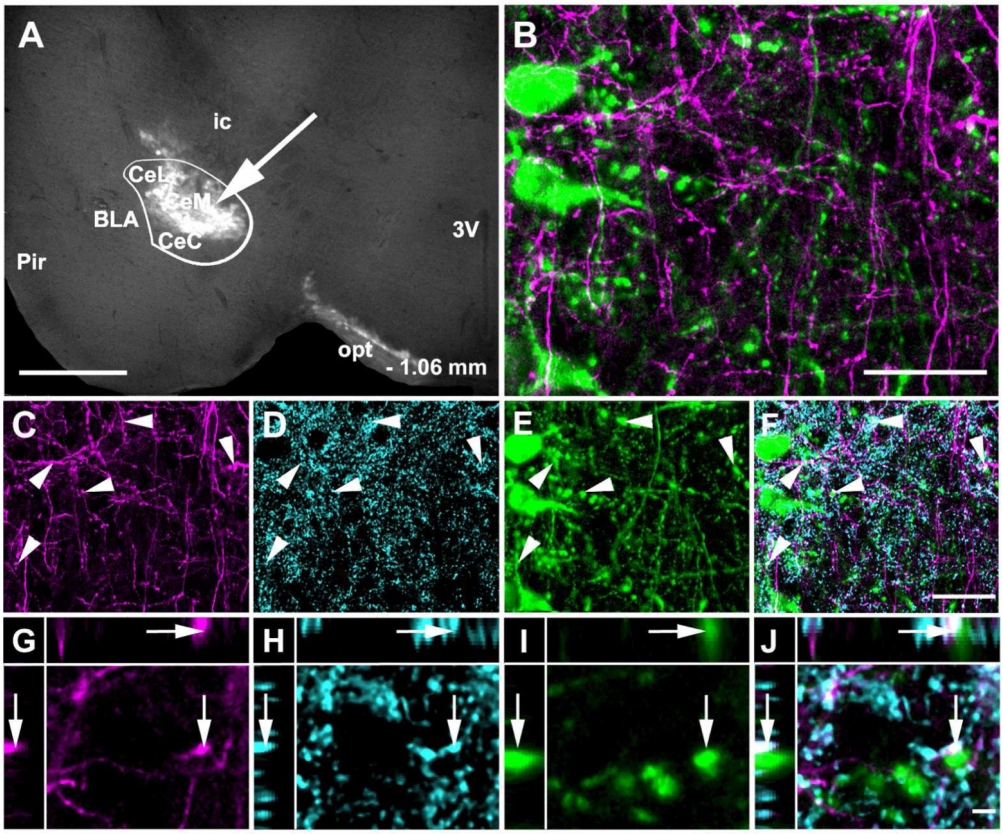

Figure 13.

Channel rhodopsin 2 (ChR2).Venus adeno-associated virus injected into the CAmy labels fibers in the LC. Panel A shows an injection site (arrow) that is concentrated in the centromedial amygdala. The white line indicates the CAmy. Panel B shows ChR2-Venus labeled fibers in the Peri-LC zone that are close to TH-ir positive neurons and fibers. ChR2-Venus fibers (C) colocalize with GAD65/67-ir (D) and are dispersed among TH-ir dendrites (E). Areas of overlap are indicated in the merged image (F, arrowheads). Possible colocalization of all three markers (ChR2-Venus; GAD65/67-ir; TH-ir) in a single optical section is shown in panels G (ChR2-Venus), H (GAD65/67-ir), I (TH-ir) and in J as a merged image. The image is presented as a XYZ image (larger panel X-Y, with Y-Z left and X-Z top). The arrow points to a puncta with possible colocalization between ChR2-Venus, GAD65/67ir and TH-ir. Abbreviations: 3V – third ventricle, BLA – basolateral amygdala, CeL – centrolateral amygdala, CeM – centromedial amygdala, CeC – centrocentral amygdala, ic – internal capsule, opt – optic tract, Pir – piriform cortex. – 1.06 mm indicates distance to bregma. Scale bar = 500 μm for A, 20 μm from B to F and scale bar = 5 μm for G to K.

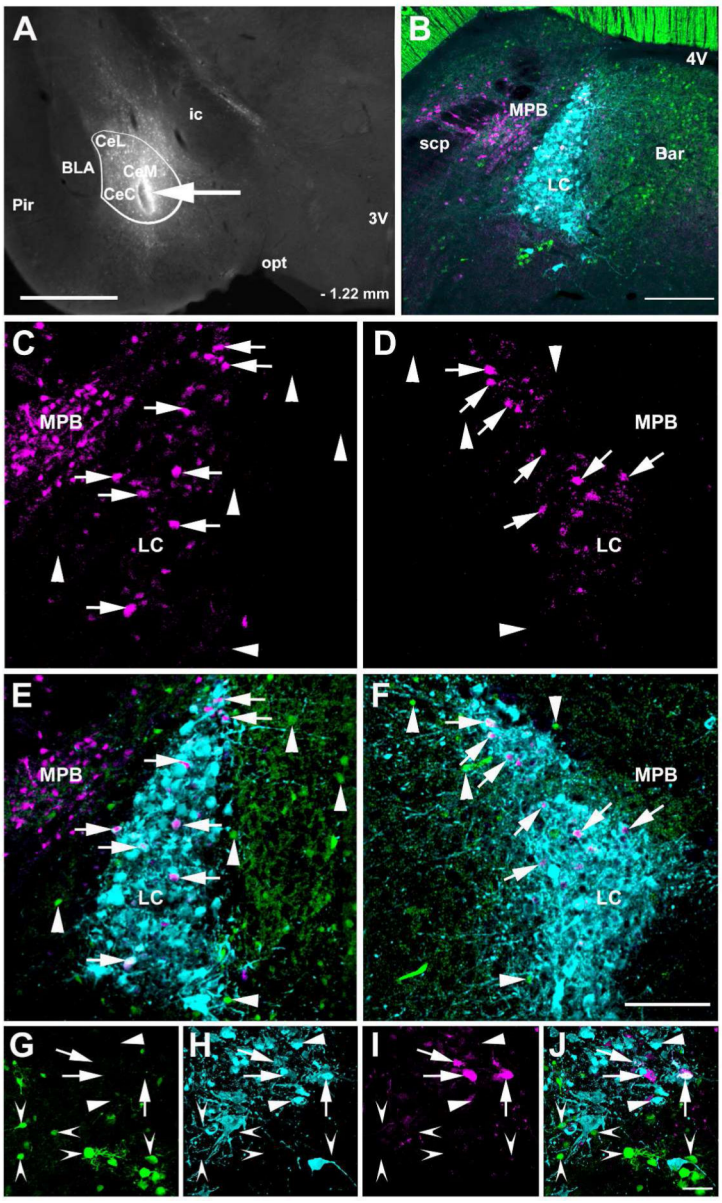

Figure 14.

Transneuronal infection of LC neurons following CAmy injection of herpes simplex 1 virus, strain H129 encoding Cre recombinase dependent tandem dimer Tomato fluorescent protein (HSV1-H129-LStdT). GABAergic neurons in the injected mouse contain Cre recombinase under control of the vesicular GABA transportr gene and a Cre recombinase activated GFP reporter (VGAT-iCre/GFP). Panel A shows a coronal section that includes the amygdala. An arrow points to the injection site and a white line delineates the CAmy. Panel B shows the general distribution of tdTomato containing cells, GABAergic neurons and TH-ir neurons and processes in the LC and Peri-LC zone 72 hours after virus injection. Panel C shows tdTomato in the ipsilateral and panel D the side contralateral to the injection at higher magnification, the images are taken from the same brain section. Panels E and F show viral tdTomato labeling merged with TH-ir and GABAergic labeling. Arrows point to tdTomato

containing TH-ir neurons in the LC. Arrowheads point to GABAergic neurons in the Peri-LC zone. Cells containing viral tdTomao are clearly visible in the medial parabrachial nucleus on side ipsilateral but not contralateral to the injection. At higher magnification arrows in panels G (GABAergic neurons), H (TH-ir neurons), I (tdTomato containing cells) and J (merged image) show overlap between LC TH-ir neurons and viral labeled cells while indented arrowheads indicate GABAergic neurons with no indication of virus infection and flat arrowheads uninfected TH-ir neurons. Abbreviations: 3V – third ventricle, 4V – fourth ventricle, Bar – Barrington nucleus, BLA – basolateral amygdala, CeL – centrolateral amygdala, CeM – centromedial amygdala, CeC – centrocentral amygdala, ic – internal capsule, LC – locus ceruleus, MPB – medial parabrachial nucleus, opt – optic tract, Pir – piriform cortex and scp – superior cerebellar pedincule. – 1.22 mm indicates distance to bregma. Scale bar = 500 μm in A and scale bar = 200 μm in B, scale bar = 100 μm in C to F and scale bar = 20 μm in G to J.

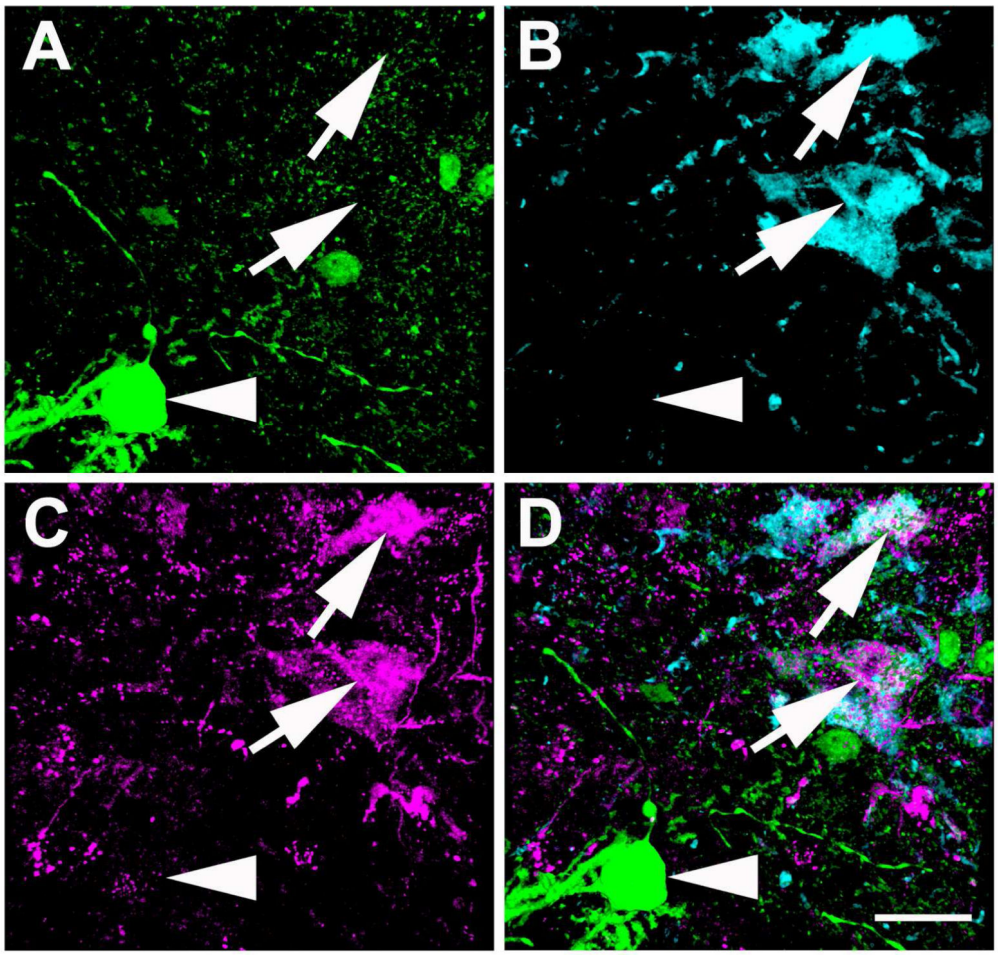

Figure 15.

High magnification image of LC TH-ir neurons labeled with HSV1-H129-LStdT after injection in the CAmy of a VGAT-iCre/GFP mouse. Panel A shows GFP expression, panel B shows TH-ir positive neurons, panel C shows HSV1-H129-LStdT labeled cells and panel D is a merged image. Arrows point to neurons that coexpress TH-ir and tdTomato from HSV1-H129-LStdT. The arrowhead points to a neighboring GABAergic neuron without a viral expression. Scale bar = 20 μm.

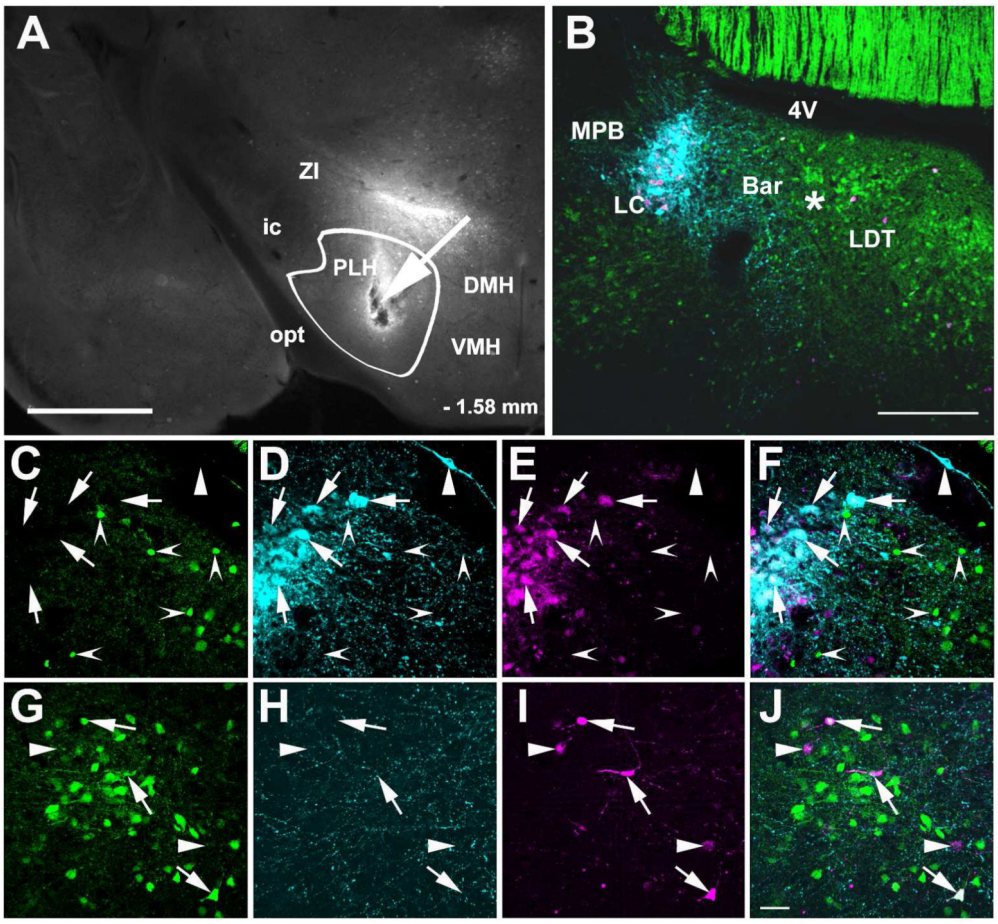

Figure 16.

Transneuronal infection of LC neurons following PLH injection of aHerpes simplex 1 virus, strain H129 encoding Cre recombinase dependent tdTomato 72 hours after the injection in a mouse that expresses Cre recombinase and GFP in GABAergic neurons. Panel A shows a coronal section in which an arrow points to the injection site within the PLH, which is delineated by a white line. Panel B shows the general distribution of tdTomato containing cells, GABAergic neurons and TH-ir in the LC area 72 hours the virus injection. Arrows in panels C (GABAergic neurons), D (TH-ir neurons and processes), E (virus infected cells) and F (merged image) indicate virus infected TH-ir neurons. An arrowhead indicates a non-infected TH-ir neuron and indented arrowheads GABAergic neurons close to the LC core, none of which are infected. In an image at the distal medial extent of TH containing dendrites arrows in panels G (GABAergic neurons), H (TH-ir processes), I (tdTomato containing cells) and J (merged image) show some GABAergic neurons with viral labeling while the arrowhead indicates a virus labeled cell without TH-ir or GABAergic labeling. Abbreviations: 4V – fourth ventricle, Bar – Barrington nucleus, DMH – dorsomedial hypothalamic nucleus, ic –internal capsule, LC – locus ceruleus, LDT – laterodorsal tegmental nucleus, MPB – medial parabrachial nucleus, opt – optic tract, VMH – ventromedial hypothalamic nucleus, ZI – zona inserta. Scale bar = 500 μm in A, 200 μm in B and scale bar = 20 μm for C to J.

Table 1

Antibodies Used in This Study. Antibody specificity was verified by the absence labeling in animals not injected with FG .

Antigen	Immunogen	Source	Dilution
Green fluorescent protein	Recombinant full-length protein	AbCam, Chicken polyclonal, ab13970	1:1000
Fluorogold	Fluorogold	Chemicon (Millipore), Rabbit polyclonal, Ab153	1:2000
GAD65/67	Recombinant full length human GAD65-GST fusion	Enzo Life Sciences, Mouse mononclonal, mAb 9A6	1:2000
Tyrosine Hydroxylase	Native rat tyrosine hydroxylase purified from pheochromocytoma	Neuromics, Sheep polyclonal, SO25000	1:1000 (indirect immunofluorescence) 1:5000 (amplification immunohistochemistry)
NeuN	Purified cell nuclei from mouse brain	Millipore, mouse monoclonal, clone A60	1:500